

	 
<p>“Novel Drilling Technology Combining Hydro-Jet and Percussion for ROP Improvement in deep geothermal drilling”</p>	<p>This project has received funding from the European Union’s Horizon 2020 research and innovation programme under grant agreement No 101006752</p>

DELIVERABLE 6.3

“Drilling fluids properties characterization and recommendation for deep geothermal hard rock application”

ABSTRACT
<p>Three different eco-friendly additives were developed to reduce friction and adjust viscosity of the selected model drilling fluids. The additives considered as friction reducers include: 1) Hybrid NanoSilica – polyhedral oligomeric silsesquioxane (POSS) with appropriate stabilities in drilling fluids 2) graphene and its derivatives, and 3) their composites. Functionalization on graphene is conducted to improve the processability and the compatibility with the selected drilling fluids. The influence of the additives on the friction performance is examined by reciprocating pin on plate testing. After testing, microscopical investigations (Alicona Infinite) of the wear tracks are performed.</p> <p>The changes in the rheological properties of fluids are discussed, with support of complementary hot rolling tests and simplified cutting transport modelling, with the perspectives of upscaling the nano-additives based fluids for deep drilling operating conditions.</p> <p>Calculation of cuttings transport with operational parameters relevant for the upper vertical part of a wellbore show significantly improved cuttings transport efficiency with the modified POSS-GO additives, and also with the GO additive at the highest concentration tested of 0.7%, due to high effective viscosity at low shear rates. The additives increase, however, also the high shear rate viscosity, and thus the pressure losses. In contrast, the POSS additive was found to provide much less improvement to the cuttings transport capacity.</p> <p>POSS nanoparticles were selected, for further Bit Rock Interaction (BRI) testing, based on their scaling ability and their significant friction reducing effect i.e., the potential for life-increasing of the drilling tools and an efficient jetting has been prioritized for improved drilling performance.</p>

Disclaimer: The present document reflects only the author’s view. The European Innovation and Networks Executive Agency (INEA) is not responsible for any use that may be made of the information it contains.

DOCUMENT TYPE:	Report
DOCUMENT NAME:	D6.3 Drilling fluids properties characterization and recommendation for deep geothermal hard rock application
VERSION:	vfinal
DATE:	2023-02-07
STATUS:	S0
DISSEMINATION LEVEL:	PU

AUTHORS, REVIEWERS			
AUTHOR(S):	Juan Yang, Bjørnar Lund, Blandine Feneuil and Alexandre Kane		
AFFILIATION(S):	SINTEF		
FURTHER AUTHORS:			
PEER REVIEWERS:	Hedi Sellami, Laurent Gerbaud, Naveen Velmurugan (ARMINES)		
REVIEW APPROVAL:	Approved	Yes	Rejected (to be improved as indicated below)
REMARKS / IMPROVEMENTS:			

VERSION HISTORY			
VERSION:	DATE:	COMMENTS, CHANGES, STATUS:	PERSON(S) / ORGANISATION SHORT NAME:
v0.1	2022-12-23	First draft	SINTEF
V1.1	2023-01-17	Minor correction	Hedi (ARMINES)
VFINAL	2023-02-07	Final version to submit	Naveen (ARMINES)

VERSION NUMBERING	
v0.x	draft before peer-review approval
v1.x	After the first review
v2.x	After the second review
vfinal	Deliverable ready to be submitted!

STATUS / DISSEMINATION LEVEL			
STATUS		DISSEMINATION LEVEL	
S0	Approved/Released/Ready to be submitted	PU	Public
S1	Reviewed	CO	Confidential, restricted under conditions set out in the Grant Agreement
S2	Pending for review		
S3	Draft for comments	CI	Classified, information as referred to in Commission Decision 2001/844/EC.
S4	Under preparation		

TABLE OF CONTENTS

1	Introduction	4
2	Synthesis of additives	5
2.1	Synthesis of POSS	5
2.2	Functionalization of graphene oxide with POSS	7
3	Characterization of drilling fluids with additives	9
3.1	Preparation of model drilling fluids with additives	9
3.2	Flow behaviour of the drilling fluids.	10
4	Tribology test of the drilling fluids with the additives	12
4.1	Friction testing of the nanofluids	12
5	Complementary evaluation of the nanoparticles as additives in the drilling fluids via hot rolling and filter press test	14
5.1	Hot rolling test	14
5.2	Filter press	16
5.3	Conclusion of the complementary experiments	17
6	Modelling of cuttings transport in vertical wellbore	18
6.1	Cuttings transport efficiency: theory	18
6.2	General theory for particle settling	18
6.3	Model for particle settling in Herschel-Bulkley fluids	20
6.4	Sample calculations	20
6.4.1	Rheological characterization	21
6.4.2	Cuttings transport efficiency : results	29
6.5	Discussion	35
7	Conclusion	35
	References	36

CONTENT

1 Introduction

The main objective of ORCHYD is to develop and demonstrate a new generation of hybrid Hydro-Percussive drilling technology able to extend the drilling performances (ROP) in very hard rock from the actual range of 1-2 m/h to a range of 4-10 m/h, according to the geological context and the drilling programme. This will be achieved by redesigning and merging two mature technologies, High Pressure Water-Jetting (HPWJ) and Percussive Drilling. In addition, developing new type of drilling fluid can also facilitate efficient breaking and transport of the rock particles, and extension of lifetime of drilling tools.

Over the past decade, various additives have been used in the drilling fluid to optimize the rheological properties, filtration control and reduce the fluid loss, shale inhibitors and thereby improving wellbore stability.

- Polymers/organic materials such as polyacrylamide, organic modified clays, poly carboxylic acid, asphaltic compounds, lignite, etc have been added to the drilling fluids [1-2]. However, most of the polymer-based materials degraded thermally and chemically at relative low temperature, which lowers their effectiveness
- A number of inorganic nanomaterials [3] such as Fe_2O_3 , nanosilica, CuO and ZnO nanoparticles, Al_2O_3 , nanoclays, and carbon nanotubes have been investigated as complementary additives to drilling fluids. The application of the nanoparticles can control the rheological properties and fluid loss and show potential to enhance the stability of shale and wellbore. However, due to specific feature of high surface area, nanoparticles are likely to form agglomerates, affecting the stability of drilling fluids. For example, Al_2O_3 nano-particles (20 nm) completely sedimented in fluids after 5 hours. Additional efforts by introducing surfactants are required to minimize the settling of the nanoparticles. The types of surfactants and their amount shall be investigated to avoid adversely affecting the viscosity and chemical stability of the fluids. In addition, the surfactants should be stable under downhole HPHT conditions.
- The recently emerging graphene and its derivatives (graphene oxide and reduced graphene oxide) have become one of the most promising additives to drilling fluids for the purpose of reducing friction during drilling operation due to their superior lubricating capability and appropriate thermal stability [4-6]. The layered structure contributes to stabilize the shale formation and reduces fluid loss. Graphene being a chemically inert material. functionalization on graphene is required in order to enhance its processability when used as additives.

In this task, we have explored eco-friendly additives with high thermal stability in an attempt to reduce friction and adjust viscosity. The additives selected as friction reducers include: 1) Hybrid Polyhedral Oligomeric Silsesquioxanes (POSS) with appropriate stabilities in drilling fluids; 2) graphene oxide (GO), and 3) POSS modified GO composites. Functionalization on graphene is conducted to improve the processability and the compatibility with the selected drilling fluids. The influence of the additives on the friction performance is examined by reciprocating pin on plate testing. The changes in the rheological properties of fluids and the

need for further characterization are discussed with the perspectives of upscaling the nano-additives based fluids for deep drilling operating conditions. Complementary experiments (e.g. hot rolling test) and numerical modelling of cutting transport properties are used to further evaluate the applicability of the additives in the drilling fluids. This study provided the basis for the selection a nanoparticles-based drilling fluid, for upscaling and further Bit Rock Interaction (BRI) testing in ARMINES's pilot unit during January 2023.

2 Synthesis of additives

2.1 Synthesis of POSS

Multifunctional Polyhedral Oligomeric Silsesquioxanes (POSS) is a hybrid organic-inorganic nanomaterial, composed of a silica cage with organic functional groups on its corners. The inorganic part is capable of giving improved mechanical properties while the functional groups may provide functionalities against wear. SINTEF Industry has established technology platforms to functionalize POSS. Functionalized POSS has been prepared through a controlled 2-step sol-gel synthesis. Well defined amino POSS with the size of 2-5 nm (shown in Figure 1) were prepared via a controlled sol gel process in the 1st step followed by functionalization through the state-of-art amine chemistry in the 2nd step. The advantage of such nanostructured molecules can offer a wide range of functionalities for tailor-made properties and applications. In addition, functionalization degree (fully or partially functionalization) can be adjusted to meet certain specific needs. Figure 2 shows an example of functionalized POSS.

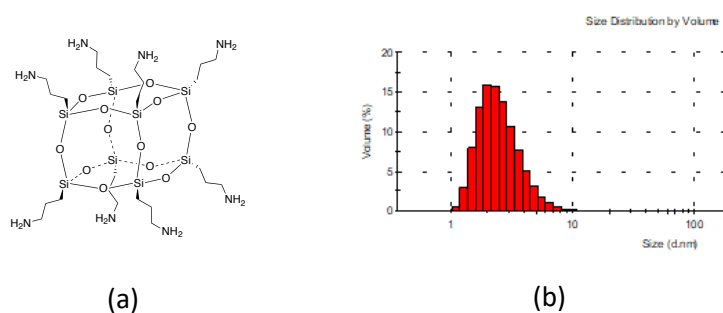


Figure 1. Amino POSS (a) and size distribution of amino POSS (b)

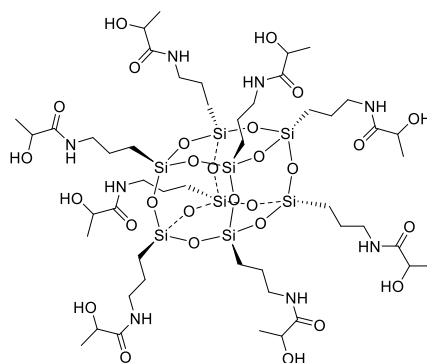


Figure 2. Example of functionalized POSS.

Nuclear magnetic Resonance (NMR) (in Bruker Avance III instrument for Liquid samples (400 MHz)) is a useful analysis tool for quality control for the functionalized POSS. Figure 3 shows a typical NMR spectrum of lactamide functionalized POSS. The Si-NMR spectra (figure 3a) indicates the cage structure dominates (over the open cage) after modification, while the peak corresponding to the formation of amide appeared in the C-NMR (figure 3b) confirms the amide functionalization was achieved successfully.

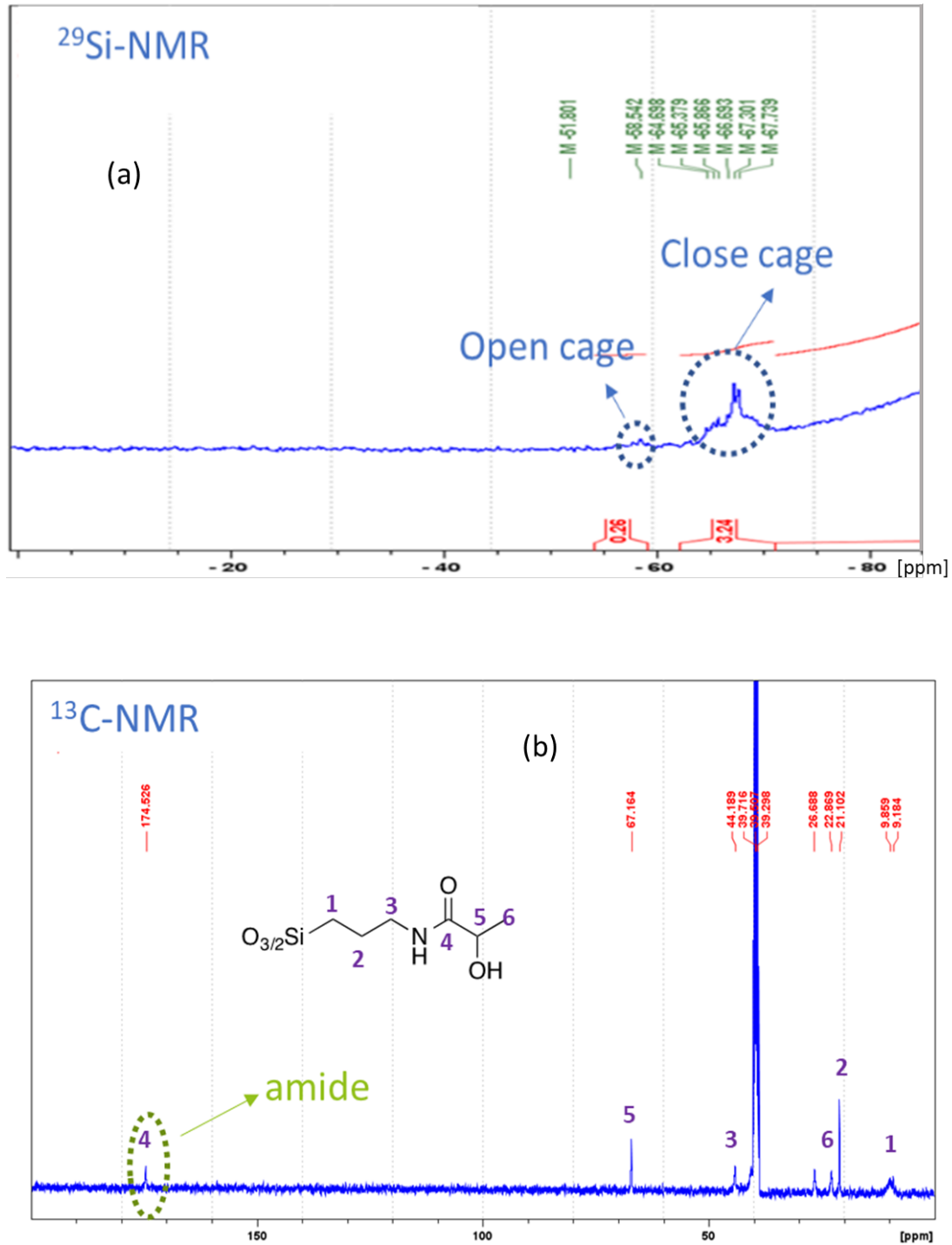


Figure 3. Typical NMR spectra for lactamide modified amino POSS.

2.2 Functionalization of graphene oxide with POSS

Graphene oxide (GO) can be functionalized via the existing functional groups e.g., carboxylic, epoxy, and hydroxyl groups. Both noncovalent and covalent bonds were used to functionalize GO with POSS through different interactions among them:

- π - π interaction between GO and POSS modified with aromatic groups.
- Covalent functionalization between POSS molecules with NH₂ or OH groups, and different functional groups on GO.

Such functionalization is expected to improve the adhesion of the GO to substrates and also dispersibility of GO with matrix or coatings, and in turn provide wear protection.

Two different POSS were used to functionalize GO

- Imine POSS with benzyl functional group for π - π interaction with GO
- 50% modified lactamide POSS and lauric POSS for covalent bonding with GO.

The functionalization procedure ended with a sufficient washing process to remove any remaining unreacted free POSS. The samples were prepared as KBr discs and characterized in transmission mode on a Bruker Vertex 70 instrument equipped with a DTGS detector. FEI Titan G2 60-300 TEM instrument equipped with EDS was used to analyse the samples. The samples were dispersed in ethanol. The dispersions were dried on copper grid.

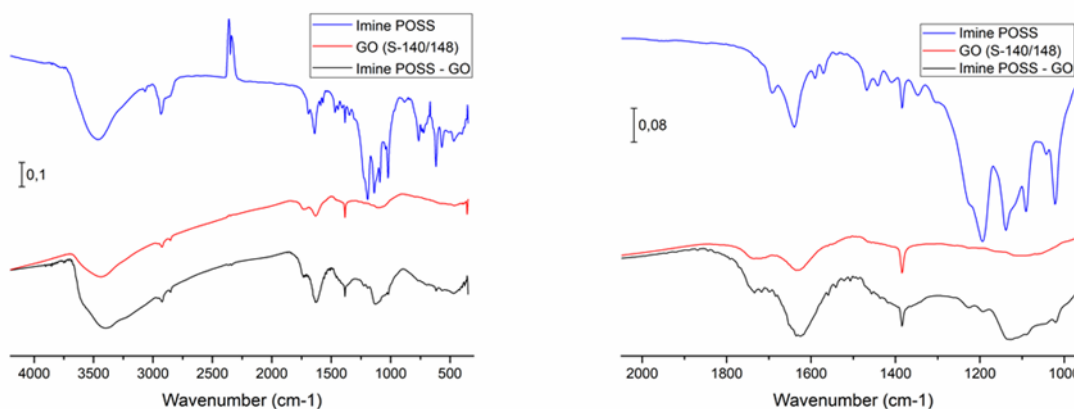


Figure 4. FT-IR spectra for imine POSS modified GO

The FTIR spectra show bands from both GO and imine POSS in the product as shown in Figure 4. A reaction product was formed and not just a mechanical mixture. The imine bands in the product are weak, which implies that the amounts of incorporated imine POSS were low. FTIR does not provide any evidence for π - π interactions. However, bands between 1000-1200 cm⁻¹ which corresponding to Si-O-Si appeared in the sample after modifications, suggesting GO was modified with imine POSS.

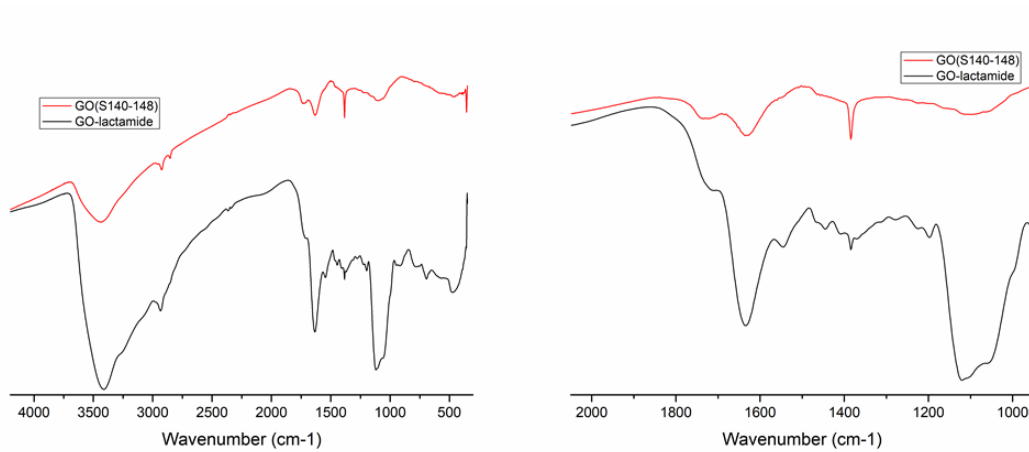


Figure 5. FT-IR spectra for lactamide POSS modified GO

Figure 5 shows the spectra of lactamide POSS modified GO and the pristine GO. The FTIR spectra show bands from GO, and a typical Si-O-Si vibration at approximately 1100 cm⁻¹ from the HAPS-core, indicating a reaction product was formed instead of a simple mechanical mixture.

The morphologies and EDS mapping imaging of functionalized GO using different POSS are illustrated in Figure 6. A relatively homogeneous distribution of silicon element on graphene sheet was observed in the whole areas in all the samples, indicating the sheets were covered by silicon-based materials (here are the different types of POSS). The TEM observation again confirms the GO were functionalized by POSS molecules. A high resolution TEM image exhibits reveals the distribution of POSS materials on the sheet of graphene oxide.

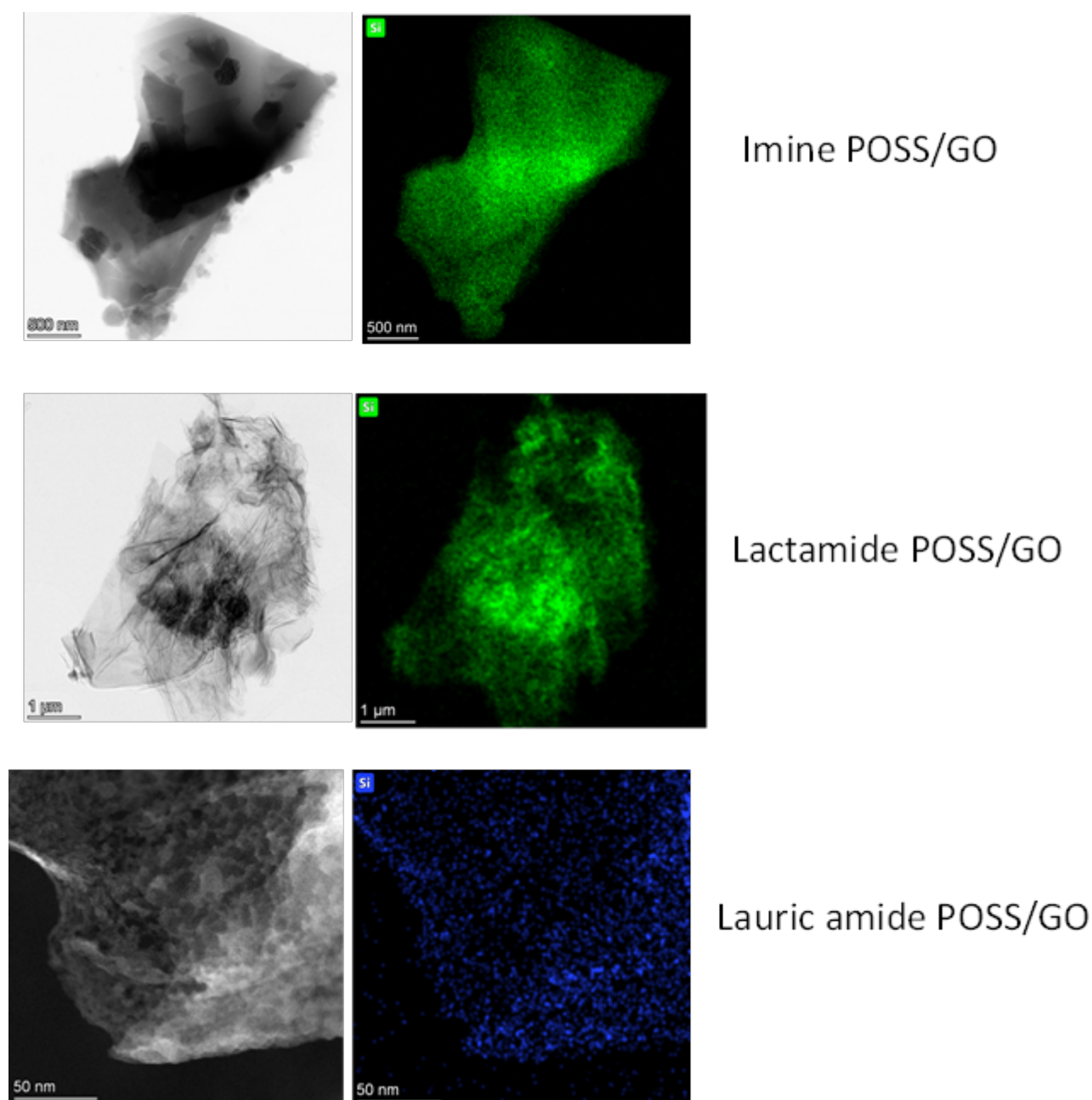


Figure 6. TEM images and EDS element mapping of the functionalized GO with different POSS

3 Characterization of drilling fluids with additives

3.1 Preparation of model drilling fluids with additives

A model drilling fluid is prepared based on the following composition: 973.27g water, 17.67g bentonite; 1.3 g xanthan gum and 7.75g Na_2CO_3 . Three different additives with different weight percentages (%) were added in the model drilling fluid, respectively shown in Table 1.

- Functionalized POSS (in house synthesized);

- GO - Graphene oxide (commercially available from Layer One, Norway);
- POSS/GO, hybrid nanosilica functionalized graphene oxide (in house synthesized).

Table 1. Compositions of drilling fluids with additives.

	GO1	GO2	GO3	POSS1	POSS2	POSS3	LAURic POSS/GO	Imin POSS/GO
GO (%)	0.10	0.35	0.70	-	-	-	-	
POSS (%)	-	-	-	1.00	1.50	2.00	-	
Lac POSS/GO (%)	-	-	-	-	-	-	0.70	
Imin POSS/GO (%)								0,70

The obtained drilling fluids were selected for different analysis: flow behaviour, tribology test and hot rolling test.

3.2 Flow behaviour of the drilling fluids.

Modular Compact Rheometer (MCR 300Anton-Paar) was used to analyse the rheological properties of the drilling fluids. The measurement was conducted at room temperature using shear rate sweeping ranging from 10–10000 s⁻¹. The measurement was conducted at two different temperatures: 20 and 50°C.

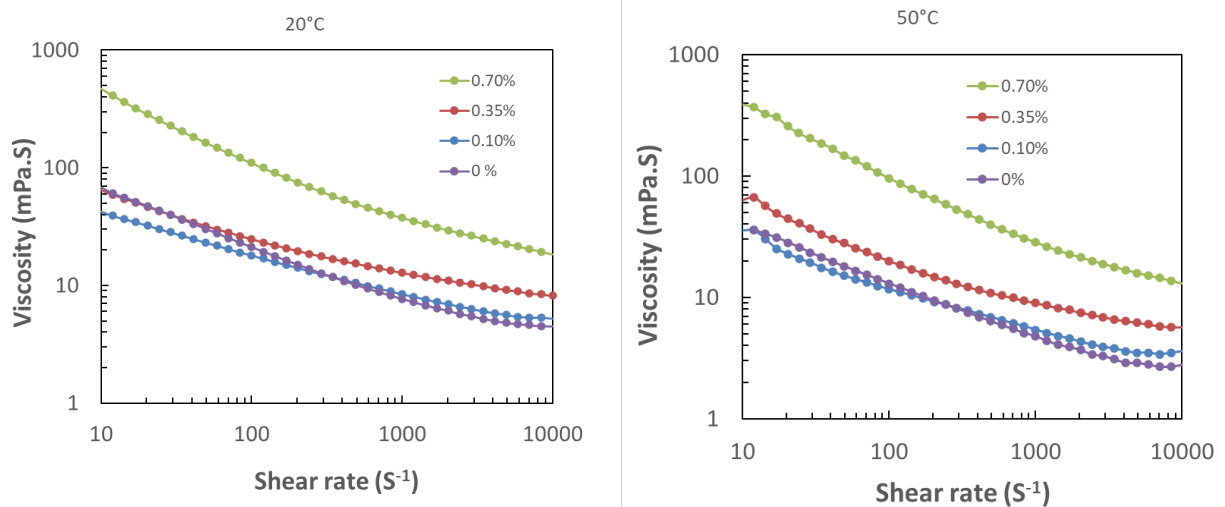


Figure 7. Plots of viscosity versus shear rate for the drilling fluids without and with GO

Figure 7 compares the flow behavior of drilling fluids with GO measured at different temperatures. All the fluids show shear thinning non-Newtonian behaviour regardless of the amount of GO. The addition of GO increases the viscosity of the drilling fluids. This increase becomes more significant when the addition reaches 0.7%. Temperatures does not impose significant change in viscosity.

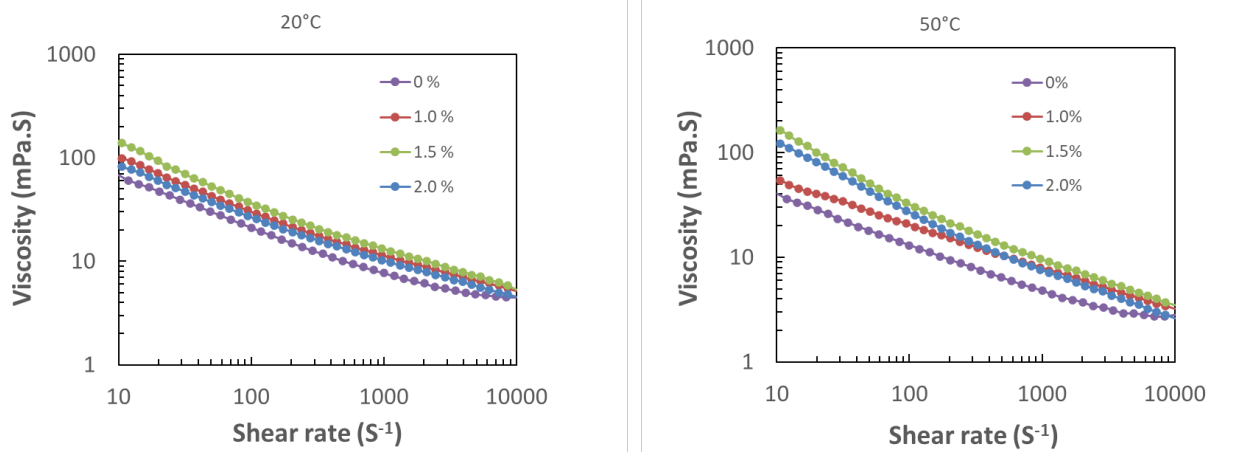


Figure 8. Plots of viscosity versus shear rate for the drilling fluids with POSS

The influence of amount of lactamide POSS as additives on the viscosity is not so dramatic as GO even when the amount is 2wt% compared with GO (0,7wt%) as shown in Figure 8. Temperature does not impose significant changes in the flow behaviour of the drilling fluids after addition of POSS. The effect of GO on the viscosity is more pronounced than that of POSS ascribed to the formation of hydrogen bonds among GO platelets. Due to the oxygen containing carbonyl, epoxy and hydroxyl groups, hydrogen bond will be formed among the GO platelets and with other drilling fluids components. This leads to an increase in the interaction among different components and to the viscosity of the fluid.

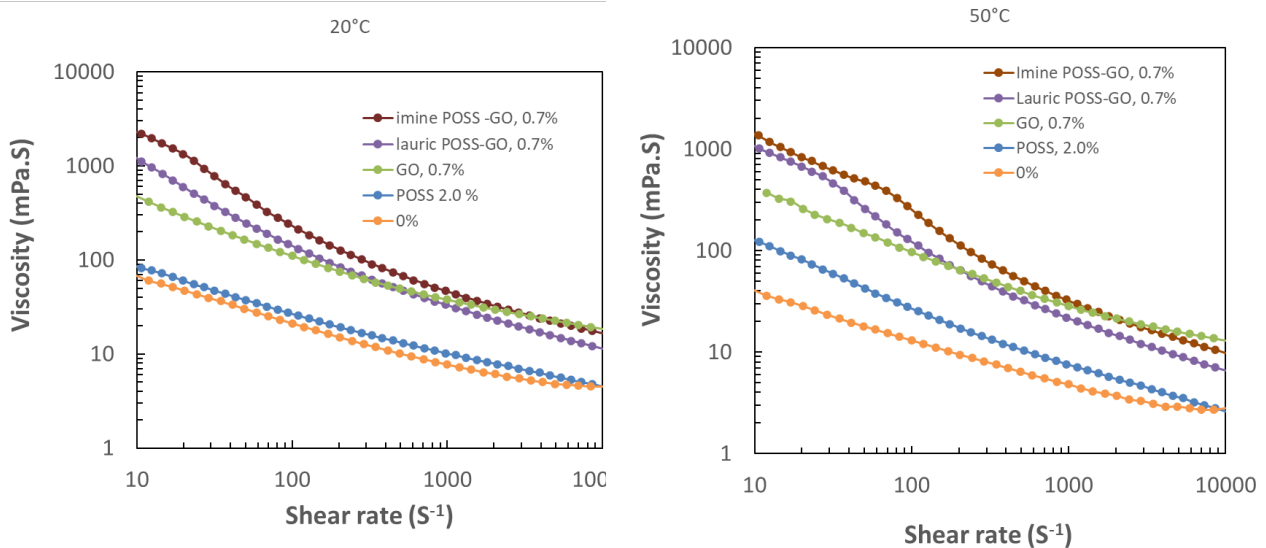


Figure 9. Plots of viscosity versus shear rate for the drilling fluids with POSS, GO and POSS-GO

Figure 9 shows the flow behaviour of drilling fluids with POSS, GO and POSS functionalized GO at 20 and 50°C. After functionalized with both imine and lauric POSS, the addition of GO increases the viscosity of the drilling fluids especially at lower shear rate compared with pristine GO. When the surface of GO has been modified with POSS, the interactions with the components of the drilling fluid might be increased and therefore increase its viscosity.

However, the enhanced interactions became less significant when the shear rate is high. The temperature has imposed some impacts on the viscosity, either increases or decreases the viscosity depending on the additives, but the change is not significant.

4 Tribology test of the drilling fluids with the additives

4.1 Friction testing of the nanofluids

The wear testing was done with a TE88 (from Phoenix Tribology) in pin-on-plate mode, in lubricated condition. An alumina ball was loaded perpendicularly to the steel plate. The normal load F_N applied was 100 N. The friction force F_f was continually measured during the test. Speed of sliding surface was 60 mm/s and the duration of test was 900 s. Two tests were performed for each fluid. The coefficient of friction is defined as $CoF = F_f / F_N$. The wear track on the samples was examined by an Alicona Infinite Microscope.

Figure 10 presents the coefficient of friction (CoF) for the drilling fluids with different additives. All the three additives decrease the CoF (compared with the reference drilling fluid), with POSS functionalized GO showing the biggest reduction of CoF. This suggests that the POSS modified GO imposed the most efficient lubricating effects. The reduction of CoF with additives was also correlated with wear track analysis of steel plates after each test (as presented in table 2). The results confirmed that all the additives reduced both width and depth of the wear track.

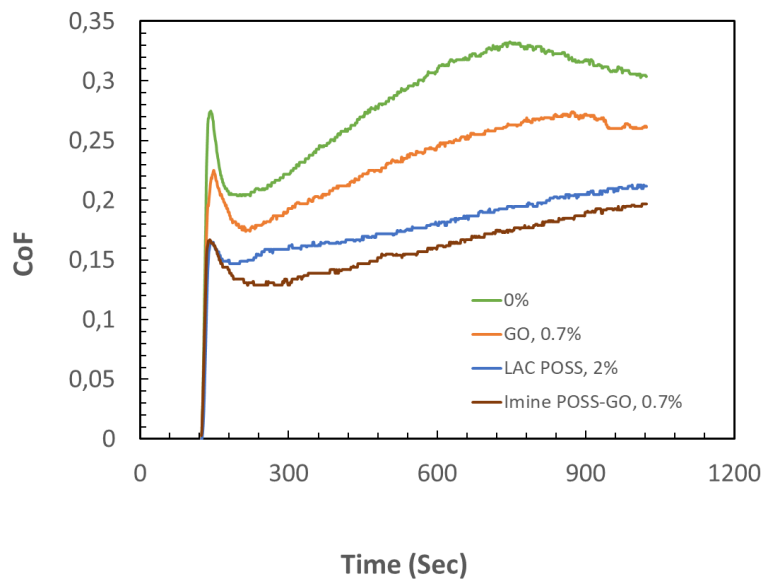


Figure 10. Influence of drilling fluid additives on the coefficient of friction.

Table 2. Width and depth of the wear tracks averaged over two tests.

samples	Width (mm)	Depth (mm)
Drilling fluids	1,100	36,5
With 0.7% GO	1,075	34,5
With 2% POSS	0,775	33,0
With Imine POSS-GO 0.7%	0,850	30,0

An Alicona Infinite Microscope was used to examine the wear track. Figure 11 compares the wear track 3D images for the drilling fluid and the one with Imine POSS-GO as additive. The results clearly showed that the wear track was narrowed after the addition of functionalized GO. The chemical functionalization on GO would probably improve the adhesion of the Imine POSS-GO on the surface forming a protection layer against further wear. The similar phenomenon was also observed in the drilling fluid with POSS, which showed superior property compared with graphene oxide. Further worn surface analysis should be conducted to confirm the explanation.

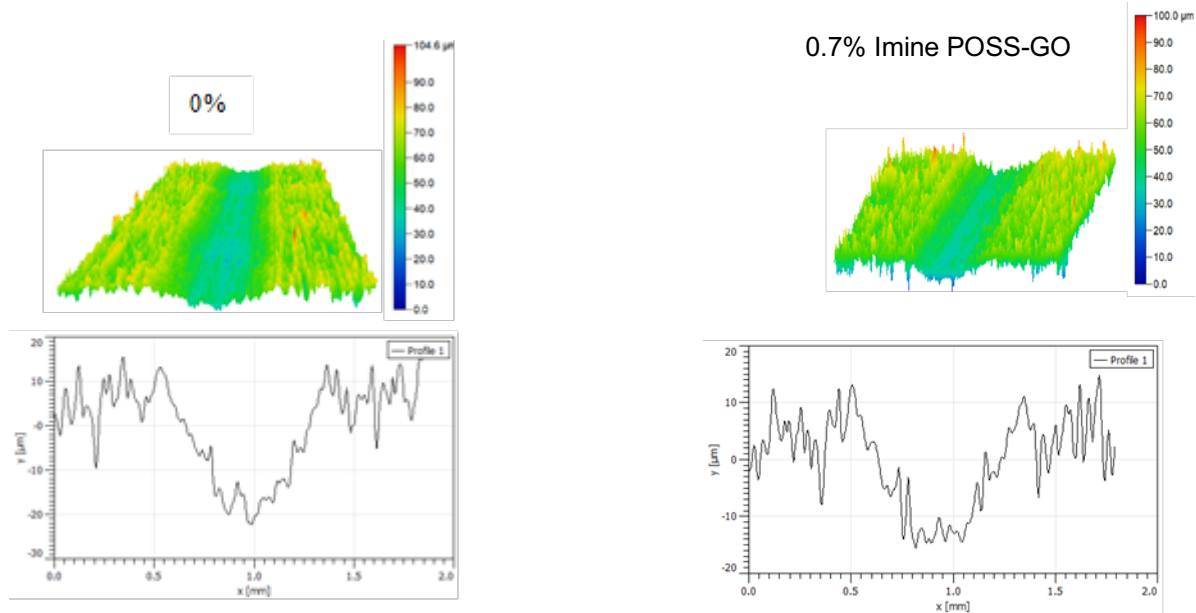


Figure 11. Micrographs and profiles of wear scars on the steel plates without and with POSS-GO as additives.

5 Complementary evaluation of the nanoparticles as additives in the drilling fluids via hot rolling and filter press test

Complementary tests were performed to get insights on the behaviour of drilling fluid containing the nanoparticles in real borehole conditions. Hot rolling experiments were carried out where the drilling fluids are exposed to high pressure and high temperature in order to evaluate (visually and by rheology tests) the fluids stability. In addition, filter press experiments were conducted to observe how fast the drilling fluids can flow across a porous rock. Only (non-functionalized) graphene oxide and POSS nanoparticles are considered for these tests. Although the POSS-GO have shown very promising friction reduction and viscosity properties, it has not been studied in this part due to its high production cost.

5.1 Hot rolling test

For hot rolling experiments, a 375-ml drilling fluid sample is poured in a 500-mL cylindrical aging cell from OFITE. Nitrogen is added to reach a pressure of 80 bar, and the cell is placed in an oven at 200°C, where it is rotated at 25 rpm for one night. Three samples have been tested: the reference drilling fluid without additives, the drilling fluid with 0.7% GO and the drilling fluid with 2% POSS.

The observations are illustrated by the pictures in Figure 12 below. The drilling fluids are stable (i.e., no phase separation) for several hours or days after preparation when no hot rolling is performed. Hot rolling induces phase separation for all three fluids:

- In the drilling fluid without additives, a small transparent layer is observed at the top of the sample after 30 min at rest (Figure 12(a))
- In the drilling fluid with GO, severe particle sedimentation is observed within very short time scales (a few seconds) (see Figure 12(b)). To understand this observation, we have observed the samples with a microscope, as shown in Figure 13. Hot rolling seems to lead to a strong aggregation of the particles, which may explain the sedimentation.
- For the sample with POSS, the aging cell wall is covered with a thick white precipitate after hot rolling. We have poured the liquid phase in a bottle and observed that the liquid separates into a transparent and a white layer within one hour. To check if the formation of precipitate is due to the POSS only, or to its interaction with the other components of the drilling fluid, we have performed an additional hot rolling experiment (70 bar, 200 °C) of a 2wt% POSS solution in deionized water. In this case, no precipitate is observed, and the solution remains colourless.

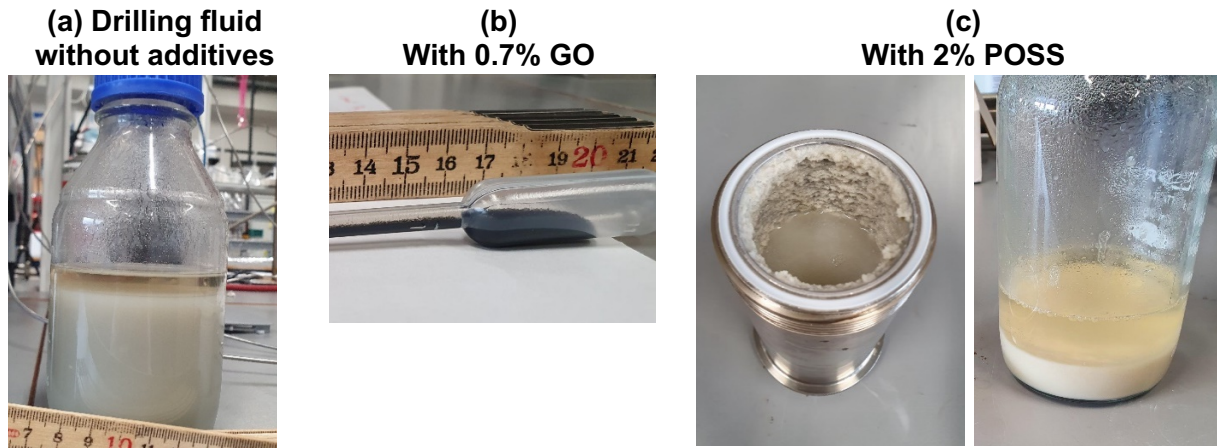


Figure 12. Pictures of drilling fluid samples after hot rolling. (a) Without additives, phase separation after 30 min at rest. (b) With 0.7% GO, particles sediment within a few seconds very fast in the pipette. (c) With 2% POSS, the aging cell wall is covered by a thick precipitate after hot rolling, and phase-separation occurs in the liquid phase after 1h.

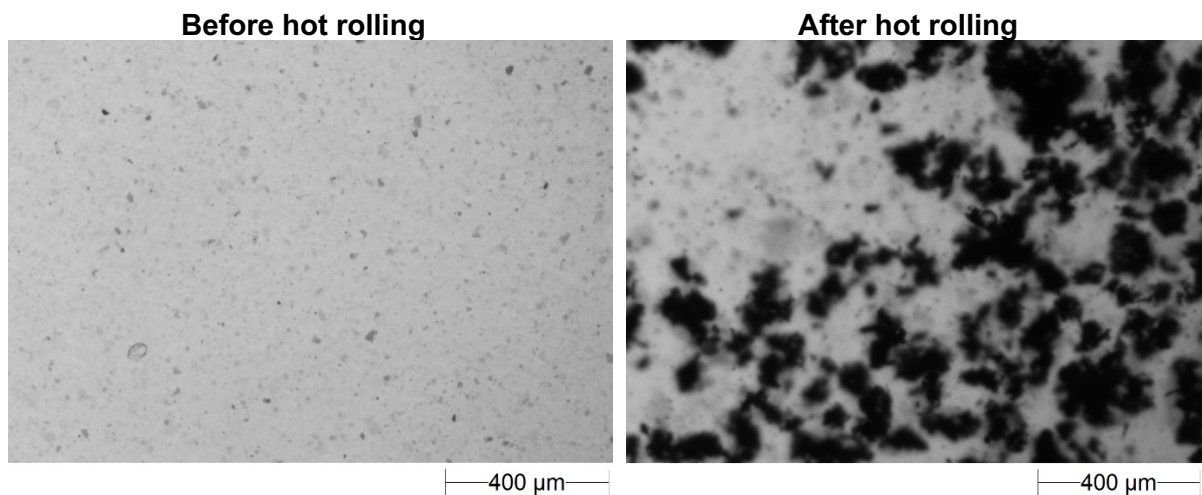


Figure 13. Microscope pictures of drilling fluid with 0.7% GO before and after hot rolling.

We have measured the rheological properties of the drilling fluids after hot rolling and compared them with the properties before temperature/pressure exposure. As the fluids tended to phase-separate, we have carefully remixed the fluid with a spatula just before the placement in the rheometer. In some cases, the maximum shear rate needed to be decreased to 1000 s^{-1} to avoid expulsion of fluid from the rheometer cell. The results are given in Figure 14. The hot rolling process tends to lead to a decrease of the viscosity, until one order of magnitude. The only cases where hot rolling increases the viscosity is the base drilling fluid and the drilling fluid with GO at very low shear rates, below 0.1 s^{-1} .

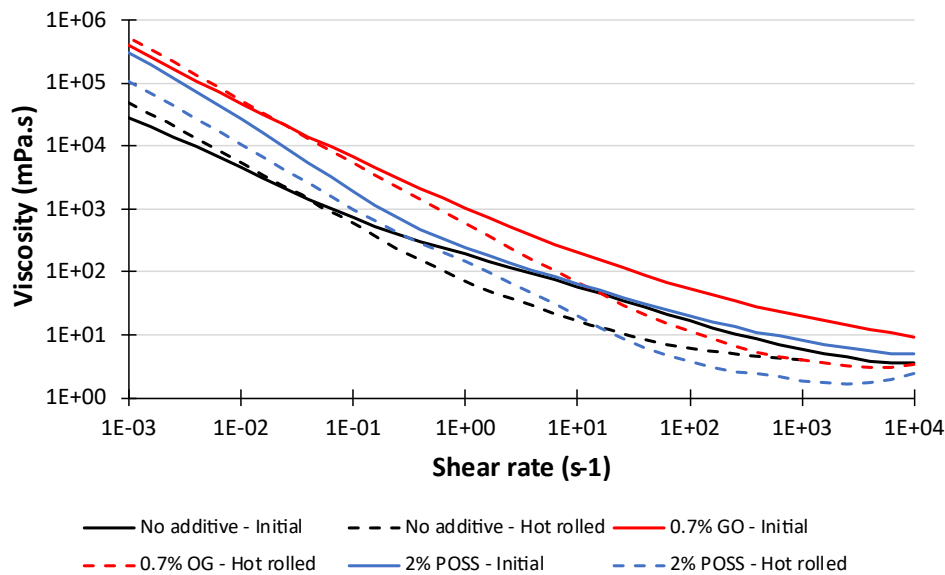


Figure 14. Effect of hot rolling on the rheological properties of drilling fluids, with and without additives.

5.2 Filter press

The filter press experiments allow to evaluate how a drilling fluid behaves when in contact with a porous rock. Two results are obtained from these tests: (1) How much liquid is lost into the porous material (fluid loss) and (2) the thickness of particles accumulated at the wall, i.e., the thickness of the filter case.

We use a filter press from OFITE. The 100 mL samples of drilling fluid are poured in the 250 mL cell. At the bottom of the cell a ceramic disk of porosity 5 microns is previously placed. The sample is heated to 150 °C before the experiment, and the temperature is maintained during the whole experiment. Pressure applied at the top of the sample (with nitrogen) is 50 bar, and pressure below the porous disk is 15 bar, giving a differential pressure of 35 bars. The volume of the lost liquid is measured first 10 seconds after the start of the experiments, then at increasing time intervals, until all the liquid is lost or for 30 min maximum. The moment when the fluid is fully removed is easily noticeable due to the impossibility to control independently bottom and top pressure (the nitrogen is crossing freely the cell).

The fluid loss as a function of time is given in Figure 15. Note that the volume of the fluid loss given in this graph may be underestimated due to evaporation or splashing, especially in cases of very fast fluid loss. For the base fluid without additives and the fluid with 2% POSS, all the fluid was lost less than 30s after the start of the experiment. The GO was able to strongly reduce the fluid loss, and after 30 min of the experiment, only half of the fluid was lost.

Filter press experiments has been performed after hot rolling only in the case of fluid containing 0.7% GO. The hot rolling inhibits the ability of the GO additive to reduce fluid loss.

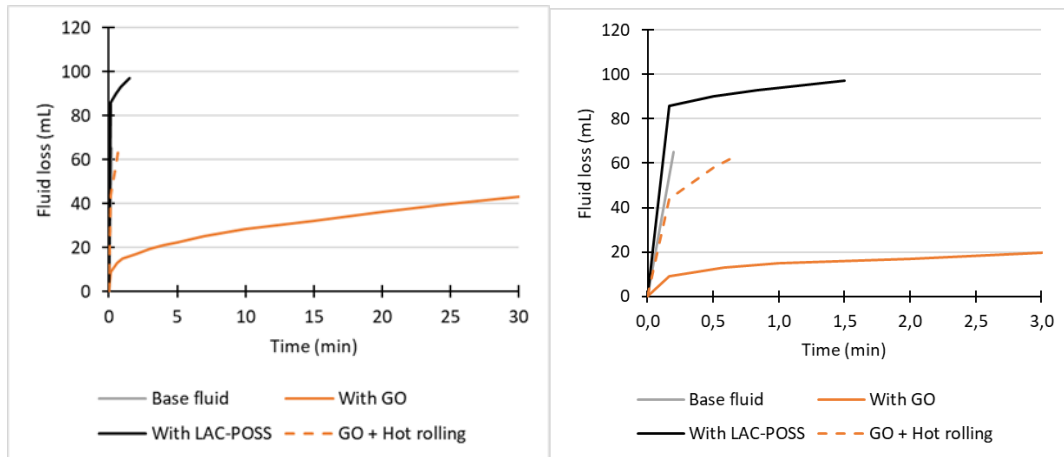


Figure 15. Fluid loss measured with filter press experiments. The graph on the left is a focus on the first minutes.

Pictures of the filter cakes are given in figure 16. For the fluid without additives and the fluid with 2% POSS, a thin filter cake (thickness below 1mm) with a lot of cracks is obtained. For the samples contained GO, before and after hot rolling, a 1-cm thick filter cake is obtained.



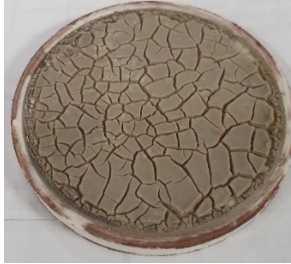

	No additives	With GO	With POSS
No hot rolling			
After hot rolling	Not performed		Not performed

Figure 16. Filter cakes obtained from the filter press experiments. The diameter of the porous ceramic disks is 5 cm.

5.3 Conclusion of the complementary experiments

Hot rolling of drilling fluids has been performed to assess the stability of the fluid under high temperature and pressure conditions. Hot rolling tends to decrease the viscosity of the fluids, by about one order of magnitude, especially at high shear rates values (above 10 s^{-1}). The change of viscosity is the same for all the drilling fluids, with and without additives, showing that this effect is mainly related to the model drilling fluid.

After hot rolling, we have also observed that the fluids tend to phase separate. A precipitate was observed in the hot rolled POSS drilling fluid. Hot rolling also made the GO particle agglomerate, leading to severe particle sedimentation.

Therefore, the effect of high pressure and temperature conditions should be further investigated, using a more suitable model drilling fluid, paying a special attention to the selection of a temperature-resistant model drilling fluid.

Regarding the filter press experiments, even if the drilling fluid without additives had very poor properties (very fast total fluid loss), the addition of GO strongly reduced the fluid loss. The POSS nanoparticles, on the other hand, had no effect on the filter press results. These observations can be explained by the size of the particles: while POSS-particles are small enough to freely cross the porous disk, the GO particles are large enough to clog the porosity. From these results, we can assume that GO-POSS particles would also improve the fluid loss.

6 Modelling of cuttings transport in vertical wellbore

We evaluate the efficiency of cuttings transport in the annulus of vertical wellbore, using field and operational data which would be typical for drilling of a deep geothermal well. Data for fluid properties are taken from experiments in this project (measurements on drilling fluids with nano particles).

6.1 Cuttings transport efficiency: theory

Cuttings transport efficiency is here defined in terms of Transport Ratio [7], which is the average transport velocity of the cuttings divided by the average annular velocity of the drilling fluid (mud), i.e.

$$T_R = \frac{U_c}{U_f} \quad (1)$$

The slip velocity U_{sl} , defined as

$$U_{sl} \equiv U_f - U_c$$

can be expressed in terms of the terminal settling velocity U_{ts0} of a single particle in an infinite quiescent fluid. Complicating factors are here

- a) geometrical effects (finite annular space)
- b) fluid-flow effects
- c) collective effects (particle-particle interactions)

We shall here only account for the latter as explained below. Thus, for a single particle we assume

$$U_{sl} \equiv U_{ts0} \quad (2)$$

6.2 General theory for particle settling

The terminal settling velocity of a single particle depends on the particle Reynolds number, defined for a Newtonian fluid as

$$Re_p \equiv \frac{\rho_f d_c U_c}{\mu_f} \quad (3)$$

where ρ_f is the fluid density, d_c is the cuttings particle diameter (or characteristic size of a particle with irregular shape), U_c is the particle velocity relative to the fluid, and μ_f is the fluid viscosity. In the limit of small particle Reynolds number, corresponding to small particles, the terminal settling velocity is given by Stokes law

$$U_{ts0} = \frac{1}{18} \frac{(\rho_c - \rho_f) g d_c^2}{\mu}; Re_p = \frac{\rho_f U_{ts0} d_c}{\mu} \ll 1 \quad (4)$$

The terminal settling velocity can generally be expressed in terms of a drag coefficient C_D which is a function of the particle Reynolds number. The settling velocity at arbitrary values of the particle Reynolds numbers can then be expressed as

$$U_{ts0} = \frac{2}{3} \sqrt{\frac{3 g d_c (\rho_c - \rho_f)}{C_D (Re_p) \rho_f}} \equiv \frac{2}{3} \sqrt{\frac{3 g d_c \Delta \rho}{C_D (Re_p) \rho_f}} \quad (5)$$

There are many published correlations for the drag coefficient. Here we use the model [8]

$$C_D = \begin{cases} \left[\sqrt{\frac{24}{Re_p}} + 0.5407 \right]^2; & Re_p < 6000 \\ 0.44; & Re_p > 6000 \end{cases} \quad (6)$$

Further, we generalize to non-Newtonian fluids by replacing the viscosity by a so-called apparent viscosity μ_a since the viscosity of non-Newtonian fluids depends on the fluid shear rate, i.e.

$$\mu_a = \frac{\tau(\dot{\gamma}_s)}{\dot{\gamma}_s} \quad (7)$$

where $\dot{\gamma}_s$ is some characteristic shear rate. The appropriate definition of $\dot{\gamma}_s$ will depend on the application. For steady particle settling it is reasonable to assume

$$\tau(\dot{\gamma}_s) \equiv \tau_s = \frac{F_{bc}}{A_c} \quad (8)$$

where F_{bc} is the buoyed weight of the cuttings particle and A_c is the particle surface area. Thus

$$\tau_s = \frac{g \frac{1}{6} \pi d_c^3 \Delta \rho}{\pi d_c^2} = \frac{g d_c \Delta \rho}{6} \quad (9)$$

Collective effects are modelled by a hindrance function $H(\phi)$, which is a function of the volumetric fraction of particles. Here we use the expression:

$$U_{ts} = H(\phi) U_{ts0} = U_{ts0} (1 - \phi)^m \quad (10)$$

with $m = 4.48$ for non-Brownian particles [9], and we approximate

$$U_{ts} \approx U_{sl} \quad (11)$$

ignoring geometric effects and effects of fluid flow on the settling velocity.

6.3 Model for particle settling in Herschel-Bulkley fluids

We here define a model for settling of an ensemble of particles with volumetric concentration ϕ in a Herschel-Bulkley fluid. A Herschel-Bulkley fluid is an inelastic, non-Newtonian fluid where the relationship between shear stress τ and shear rate is given by (for linear shear flow)

$$\begin{aligned} \tau(\dot{\gamma}) &= \tau_y + K\dot{\gamma}^n; \dot{\gamma} \geq 0 \\ \dot{\gamma} &= 0; \tau(\dot{\gamma}) \leq \tau_y \end{aligned} \quad (12)$$

where the yield stress τ_y , consistency index K and flow behaviour index n are the parameters of the HB model. This means that the fluid does not flow unless the shear stress is greater than τ_y . Drilling fluids generally have a non-zero value of τ_y and are shear-thinning, i.e. the flow behaviour index n is less than unity.

This also means that the slip velocity will be zero if the yield stress is larger than τ_s defined in eq. (9).

6.4 Sample calculations

We calculate the cuttings transport ratio for different combinations of fluid properties, particle properties, wellbore diameters and operational conditions (flow rates and drilling rates).

Herschel-Bulkley parameters have been calculated based on the rheological characterization (Chapter 3.2) and are listed in Tables 4 and 5.

Other input data are listed in Table 3. For all cases we have assumed a drillpipe diameter D_p of 5.5" (0.1397 m). This is a standard drillpipe diameter. Typical wellbore diameters are in the range from 8" to 26". We have here considered the largest size of 26" which will correspond to the lowest fluid velocities and thus to the worst case with respect to cuttings transport.

The drilling rate (rate of penetration or ROP) generates a volume flux Q_c of cuttings to be transported up the well, given by

$$Q_c = \frac{\pi}{4} D_w^2 \cdot ROP \cdot (1 - \phi) = A_w \cdot ROP \cdot (1 - \phi) \quad (13)$$

where D_w is the wellbore diameter and ϕ is the porosity of the rock. When the volumetric fluxes Q_c of particles (cuttings) and Q_f of drilling fluid are known, in addition to the slip velocity, defined by **Error! Reference source not found.**, the volumetric concentration ϕ can be calculated from

$$U_{sl} = U_f - U_c = \frac{U_{fs}}{1 - \phi} - \frac{U_{cs}}{\phi} \quad (14)$$

where the superficial velocities are defined in terms of the volumetric rates and the annular area A_a ;

$$U_{fs} = \frac{Q_f}{A_a}; U_{cs} = \frac{Q_c}{A_a} \quad (15)$$

Thus,

$$T_R = \frac{U_c}{U_f} = \frac{U_f - U_{sl}}{U_f} = 1 - \frac{U_{sl}}{U_f} \quad (16)$$

The transport ratio can be rewritten as

$$T_R = \frac{U_c}{U_f} = \frac{U_f - U_{sl}}{U_f} = 1 - \frac{U_{sl}}{U_f} \quad (17)$$

Table 3. Constant parameters used in calculations.

Symbol	Name	Value
D_w	Wellbore diameter	26" = 0.660" = 0.6604 m
D_p	Drillpipe diameter	5.5" = 0.1397 m
d_c	Characteristic cuttings diameter	2.7 mm
ρ_c	Cuttings particle mass density	2700 kg/m ³
ρ_f	Drilling fluid mass density	1000 kg/m ³
ϕ	Rock porosity	0.1
ROP	Drilling rate (Rate Of Penetration)	8 m/hr = 0.0022 m/s
Q_f	Fluid rates	3000 – 5000 liter/minute

6.4.1 Rheological characterization

The rheological properties of the fluids have been characterized based on the flow curves of shear stress versus shear rate, using the Herschel-Bulkley model (see eq. 13). This model, described above, is the de facto standard rheological model for drilling fluids.

In this work the Herschel-Bulkley parameters have been extracted from the flow curves by first determining the yield stress τ_y and then the consistency index K and the flow behaviour index n were determined by fitting the modeled shear stress to the measured shear stress at two shear rates γ_x and γ_s which are representative for the flow in question (see [10]).

Calculated Herschel-Bulkley parameters are presented in Tables 4 and 5, and measured and modeled flow curves are presented in Figures 17 through 28. It was found that for the drilling fluids with GO and for the POSS fluids the Herschel-Bulkley model fit well to the experimental data. For these fluids the yield stress was obtained by linear extrapolation down to zero shear rates, and the K and n parameters were determined by fitting at $\gamma_s = 200 \text{ s}^{-1}$ and $\gamma_x = 100 \text{ s}^{-1}$. In contrast, the Imine POSS/GO and Lauric POSS/GO fluids had a deviating behaviour at low shear rates, with a local maximum. This behavior could be due to gelling effects which can occur depending on the rheology measurement protocol. The flow curve measurements were conducted with increasing shear rates, and the maximum could be due to breaking of a gel structure which is built at zero and low shear rates.

Table 4. Herschel-Bulkley parameters for drilling fluid with GO, from measured flow curves.
The fluid labelled 0% is the base fluid without any additives.

Fluid name	Conc. GO %	20 C			50 C		
		K [Pa*s ⁿ]	n [-]	τ_y [Pa]	K [Pa*s ⁿ]	n [-]	τ_y [Pa]
0%	0	0.090571	0.62971	0.47408	0.048079	0.66264	0.28321
GO 0.1%	0.10	0.055684	0.72624	0.22162	0.055822	0.66069	0
GO 0.35%	0.35	0.065631	0.75578	0.33862	0.14216	0.57413	0
GO 0.7%	0.70	0.36213	0.65195	3.6994	0.84128	0.49579	1.3488

Table 5. Herschel-Bulkley parameters for drilling fluids with POSS and with GO modified with POSS, from measured flow curves.

Fluid name	Conc. additive %	20 C			50 C		
		K [Pa*s ⁿ]	n [-]	τ_y [Pa]	K [Pa*s ⁿ]	n [-]	τ_y [Pa]
POSS 1.0%	1	0.26863	0.52527	0	0.13737	0.58496	0
POSS 1.5%	1.5	0.36484	0.49906	0	0.47617	0.41292	0.011537
POSS 2.0%	2	0.22524	0.53616	0	0.47074	0.37696	0
LauricPOSS &GO 0.7%	0.70	0.31304	0.62253	8.4911	3.2503	0.16088	5.3748
IminePOSS &GO 0.7%	0.7	0.46915	0.54941	17	1.6718	0.35265	11

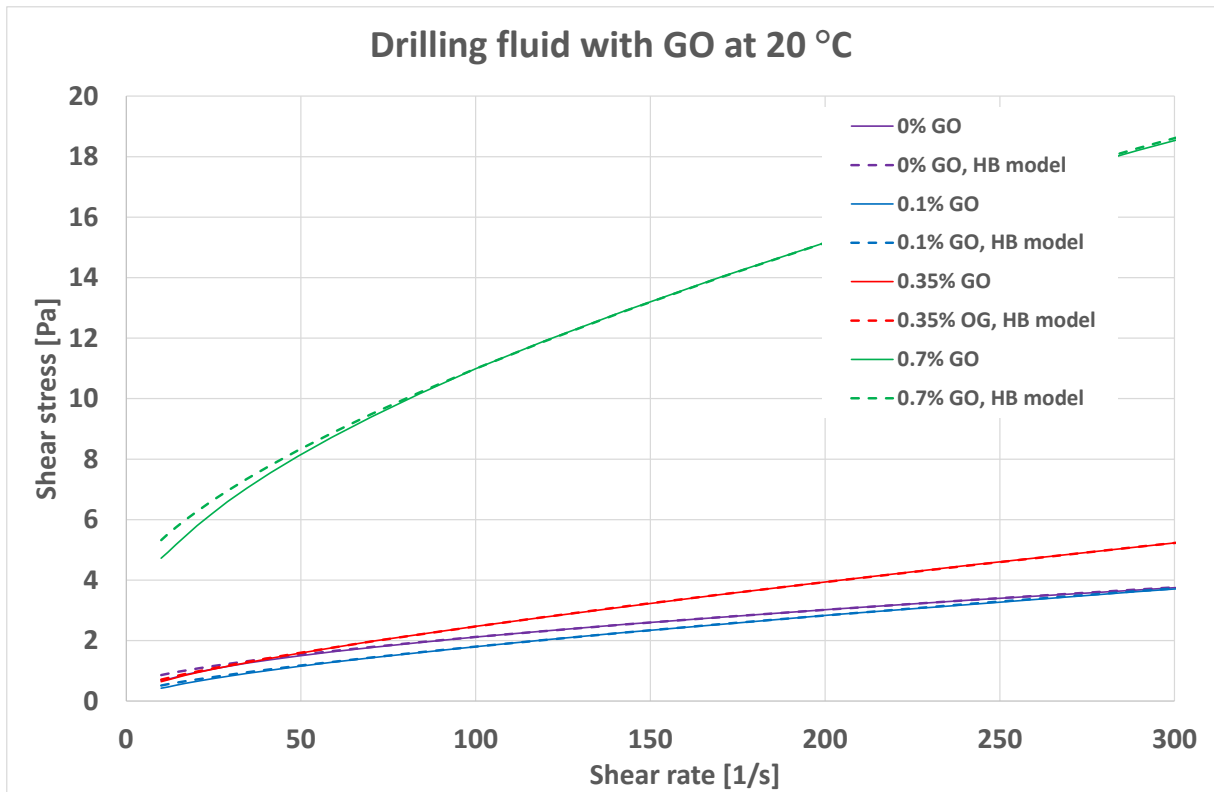


Figure 17. Flow curves from measurements (solid lines) and Herschel-Bulkley model (dashed lines) for drilling fluid with different concentrations of GO at 20 °C.

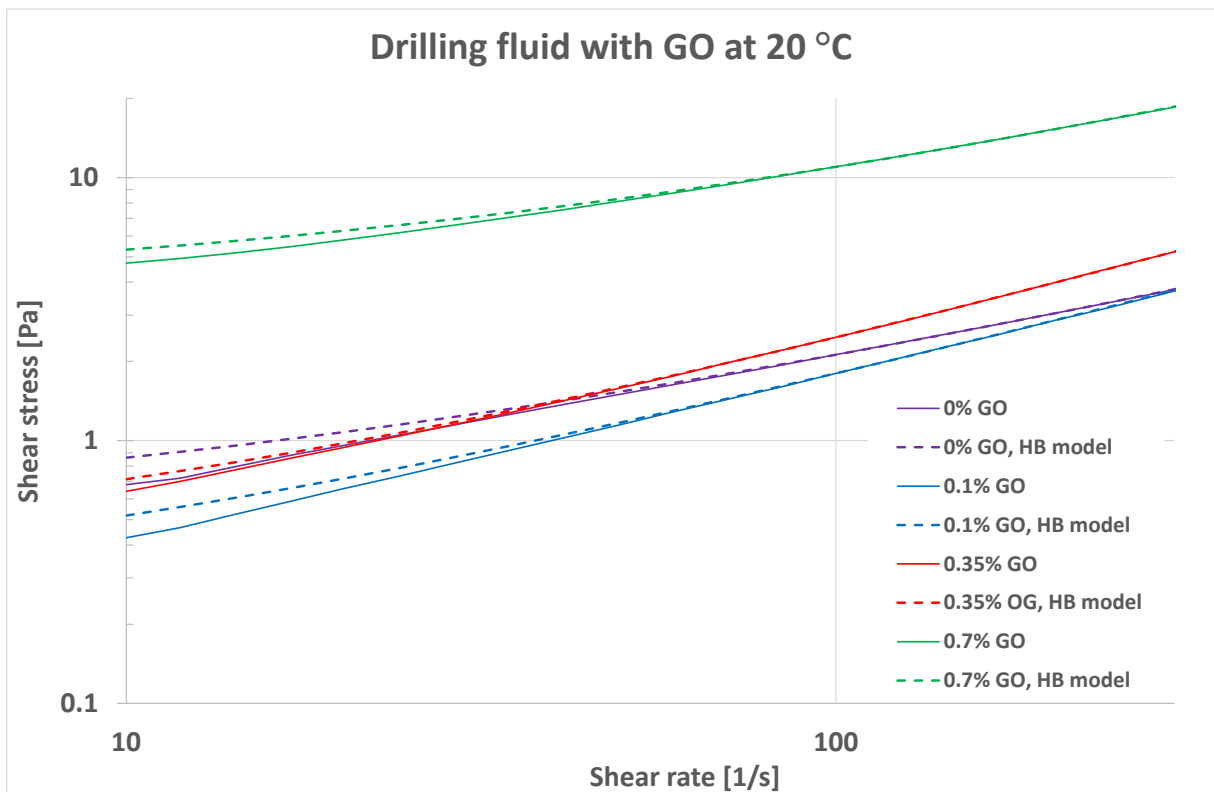


Figure 18. Flow curves from measurements (solid lines) and Herschel-Bulkley model (dashed lines) for drilling fluid with different concentrations of GO at 20 °C.

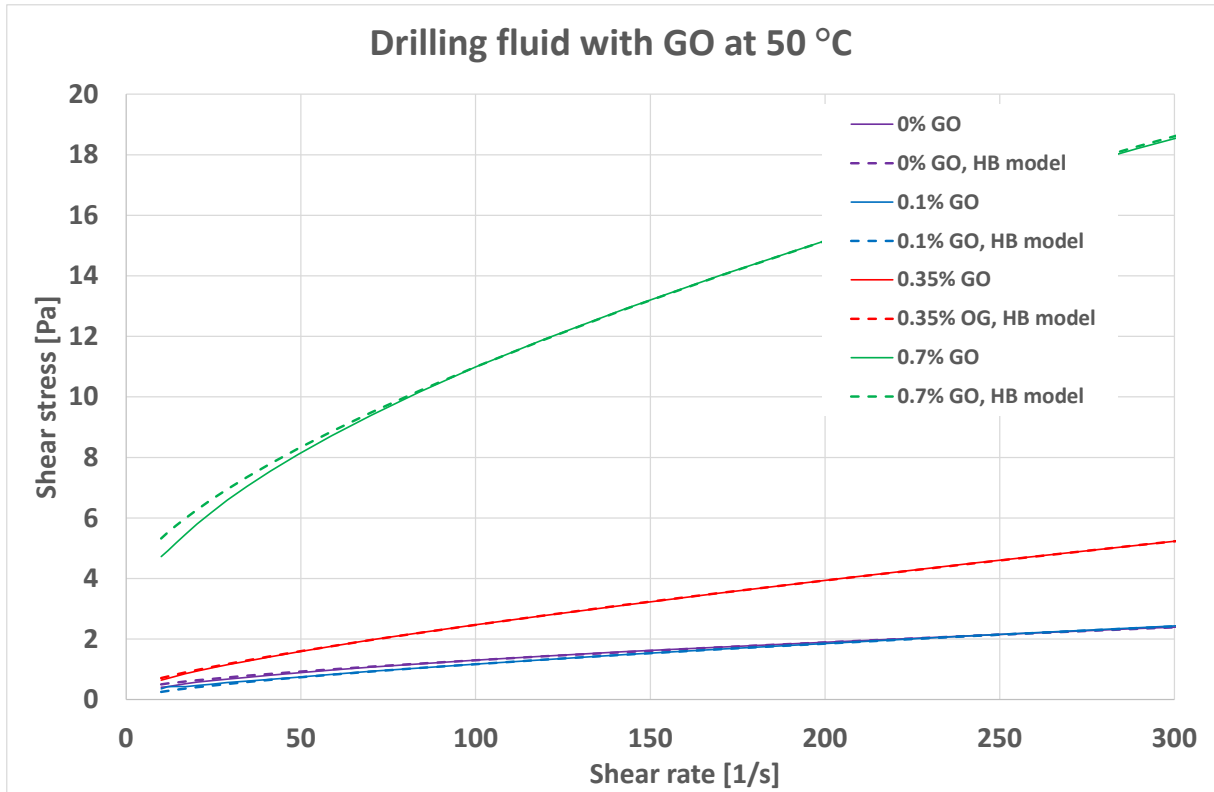


Figure 19. Flow curves from measurements (solid lines) and Herschel-Bulkley model (dashed lines) for drilling fluid with different concentrations of GO at 50 °C.

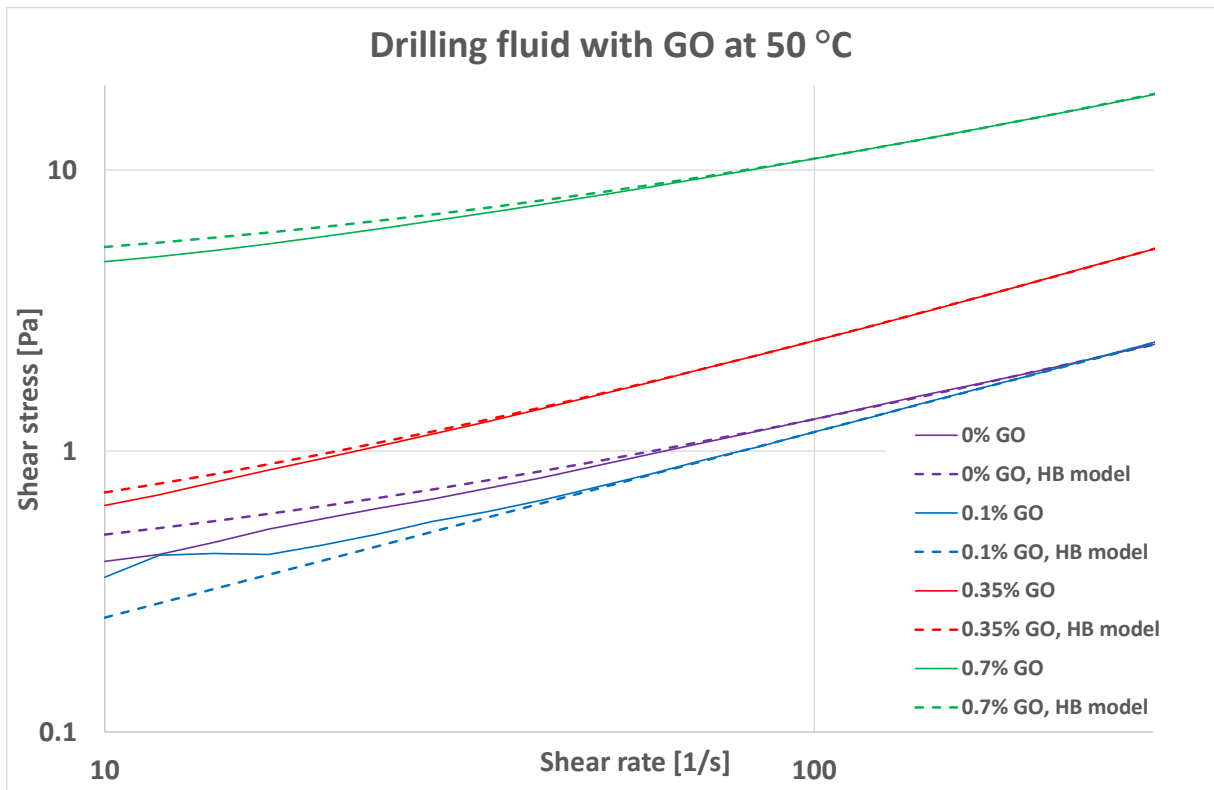


Figure 20. Flow curves from measurements (solid lines) and Herschel-Bulkley model (dashed lines) for drilling fluid with different concentrations of GO at 50 °C.

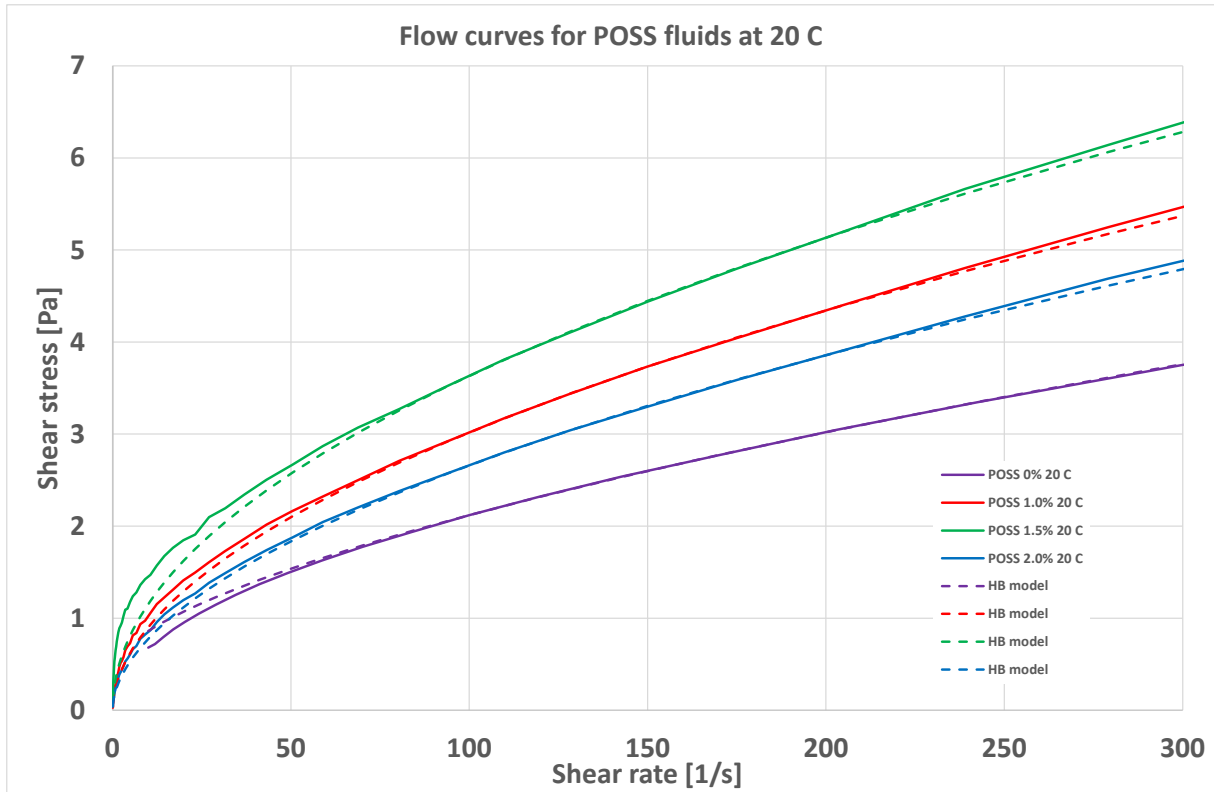


Figure 21. Flow curves from measurements (solid lines) and Herschel-Bulkley model (dashed lines) for drilling fluid with different concentrations of POSS at 20 °C.

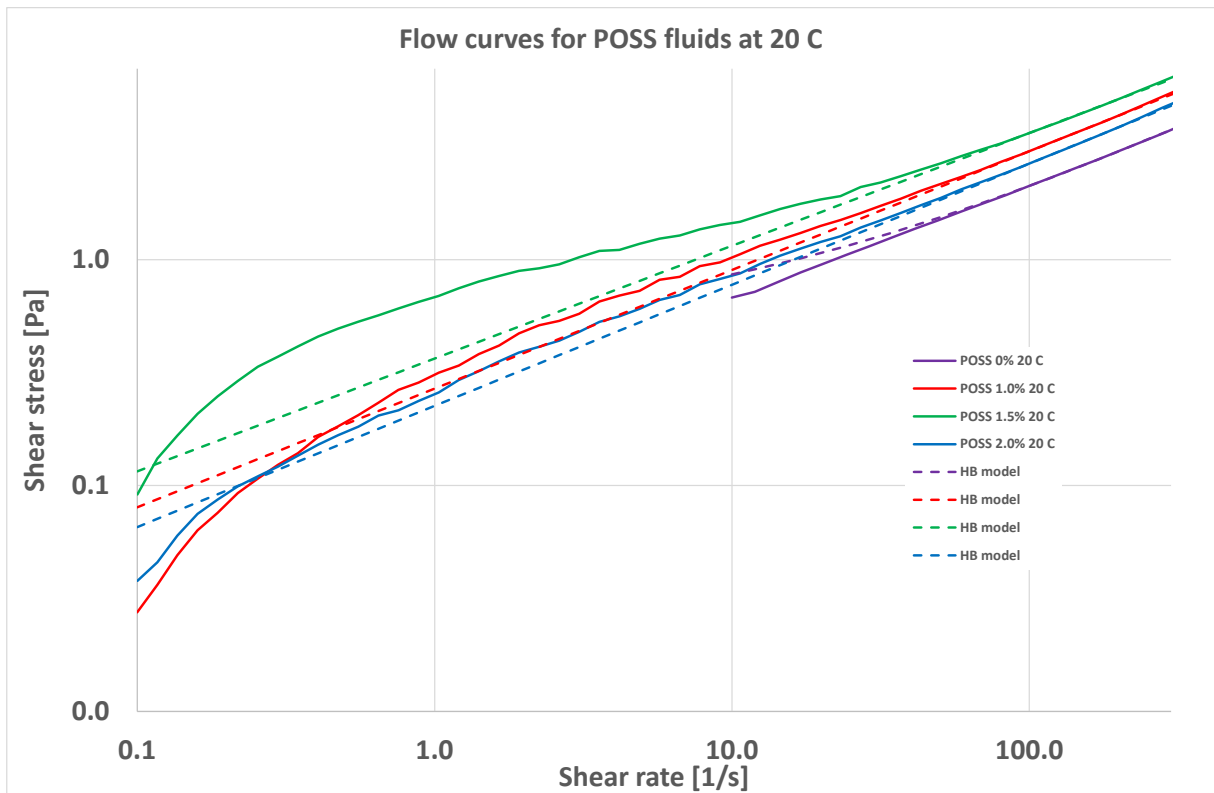


Figure 22. Flow curves from measurements (solid lines) and Herschel-Bulkley model (dashed lines) for drilling fluid with different concentrations of POSS at 20 °C.

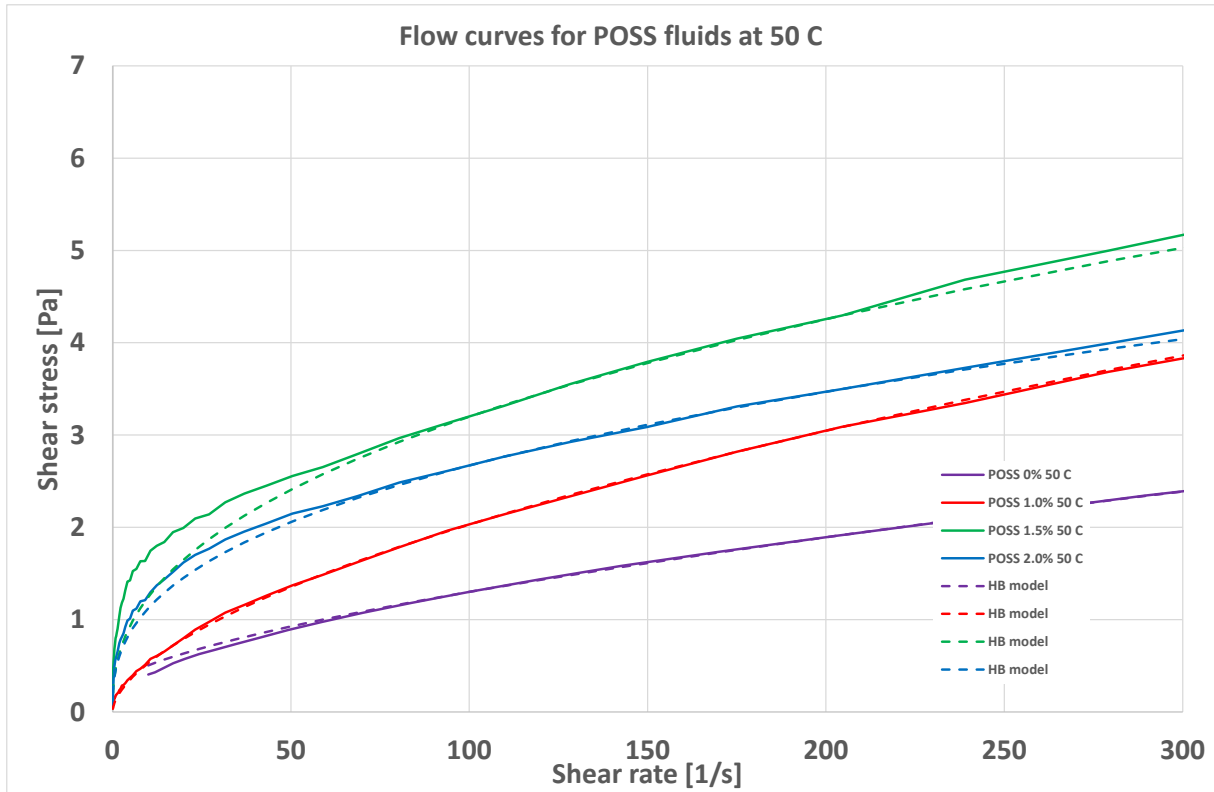


Figure 23. Flow curves from measurements (solid lines) and Herschel-Bulkley model (dashed lines) for drilling fluid with different concentrations of POSS at 50 °C.

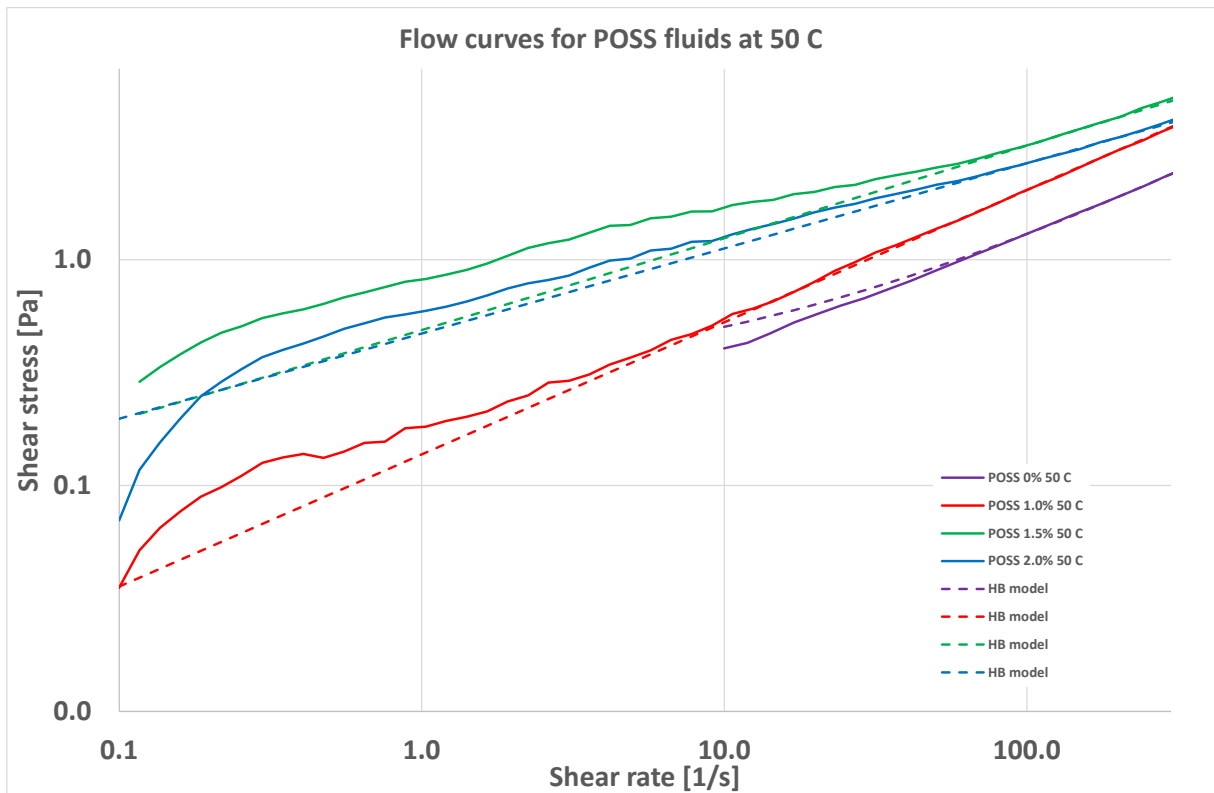


Figure 24. Flow curves from measurements (solid lines) and Herschel-Bulkley model (dashed lines) for drilling fluid with different concentrations of POSS at 50 °C.

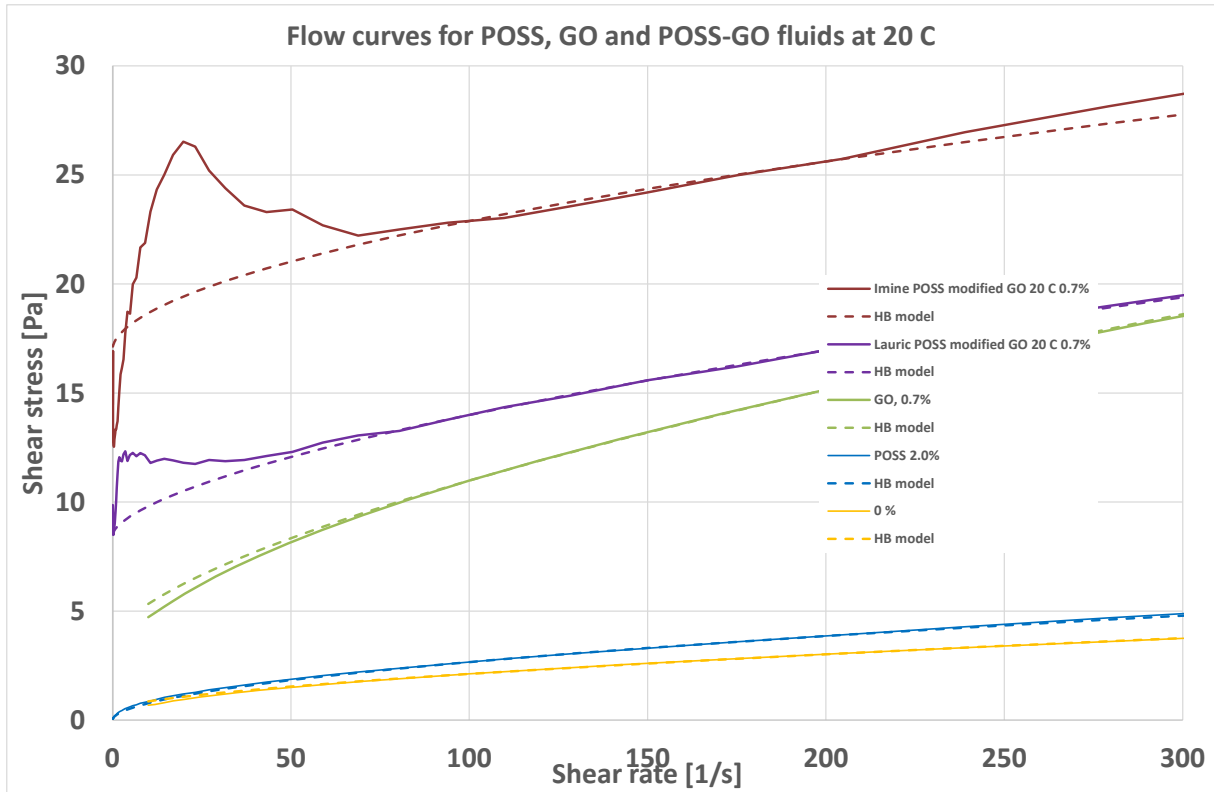


Figure 25. Flow curves from measurements (solid lines) and Herschel-Bulkley model (dashed lines) for POSS, GO and POSS-GO fluids at 20 °C.

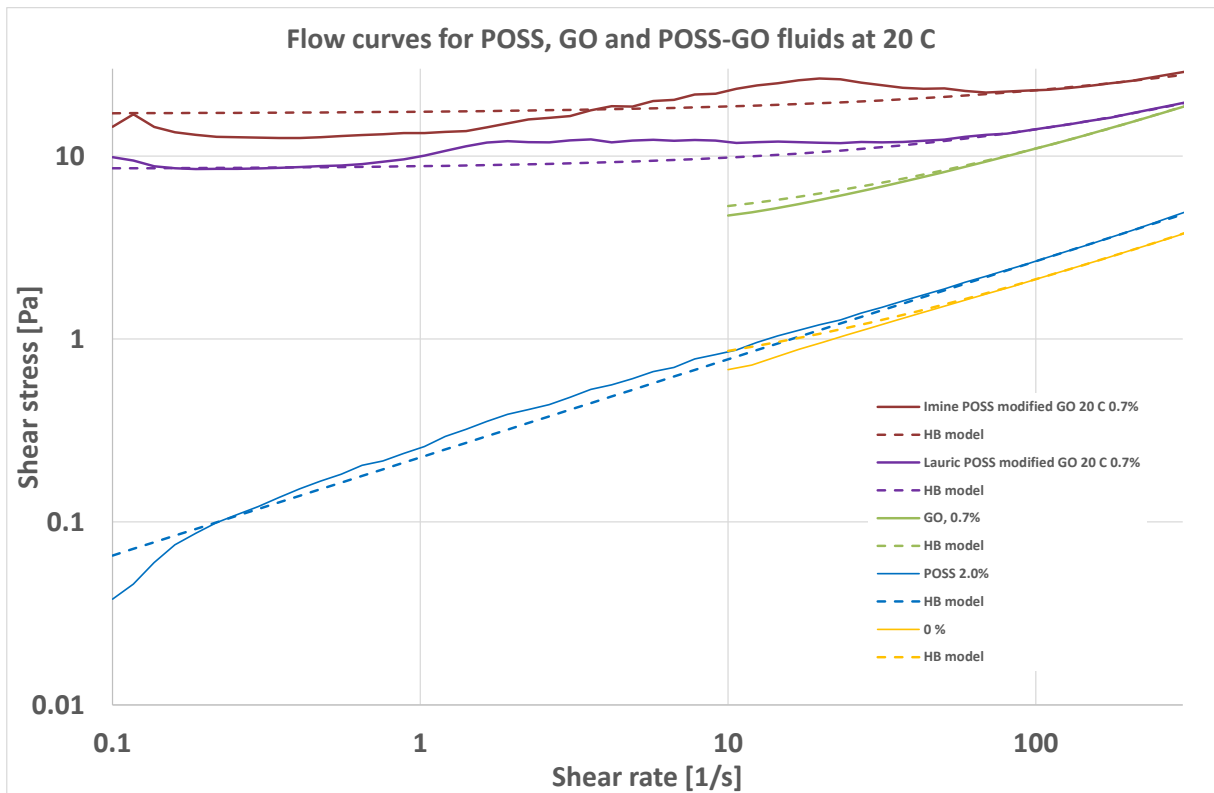


Figure 26. Flow curves from measurements (solid lines) and Herschel-Bulkley model (dashed lines) for POSS, GO and POSS-GO fluids at 20 °C.

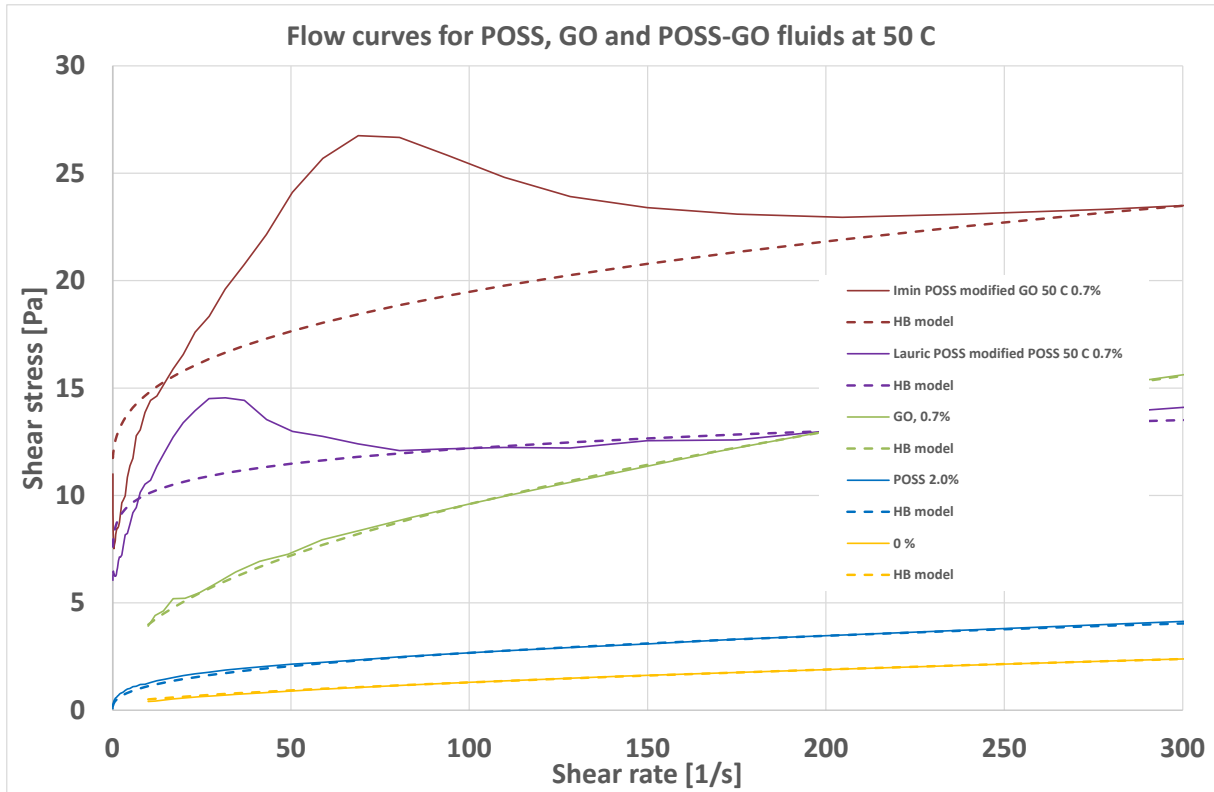


Figure 27. Flow curves from measurements (solid lines) and Herschel-Bulkley model (dashed lines) for POSS, GO and POSS-GO fluids at 50 °C.

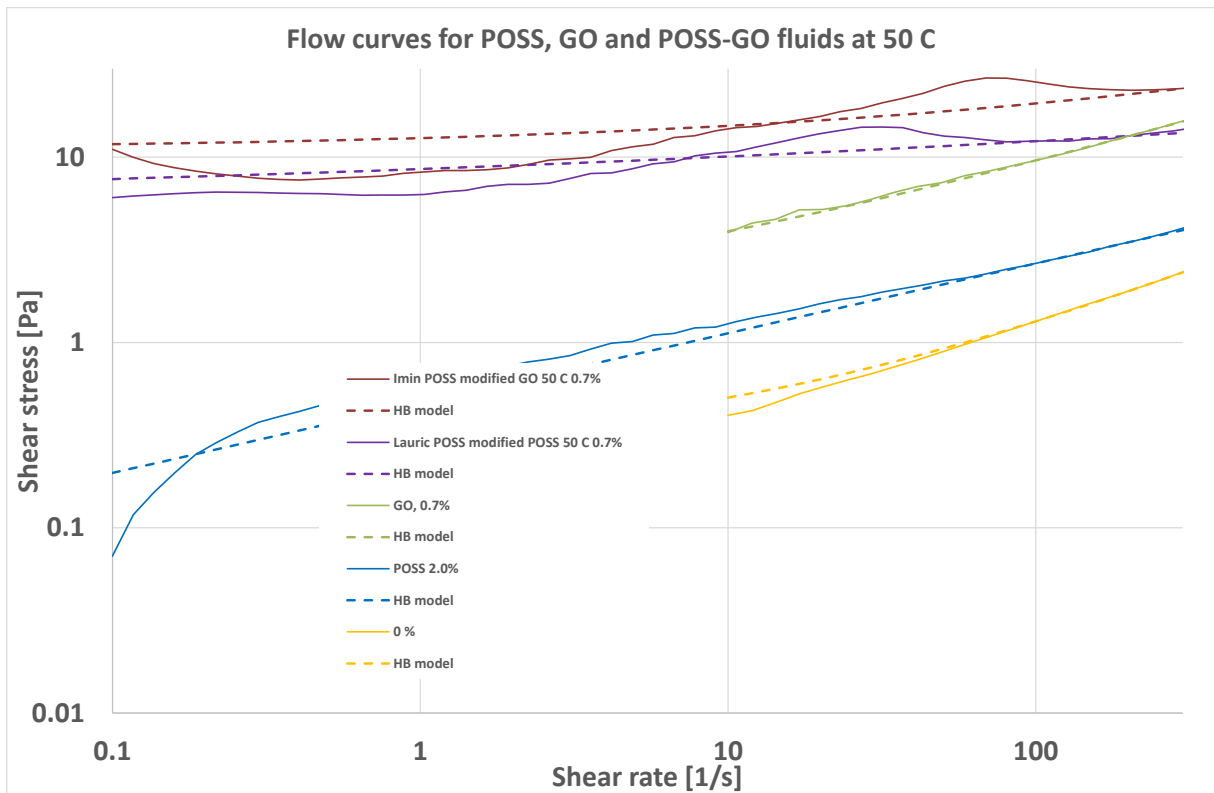


Figure 28. Flow curves from measurements (solid lines) and Herschel-Bulkley model (dashed lines) for POSS, GO and POSS-GO fluids at 50 °C.

6.4.2 Cuttings transport efficiency : results

In Figures 29 through 40 below we present graphically the results from the calculations of transport ratio and cuttings holdup for the fluids investigated, both at 20 C and 50 C, based on the model and case data set defined above.

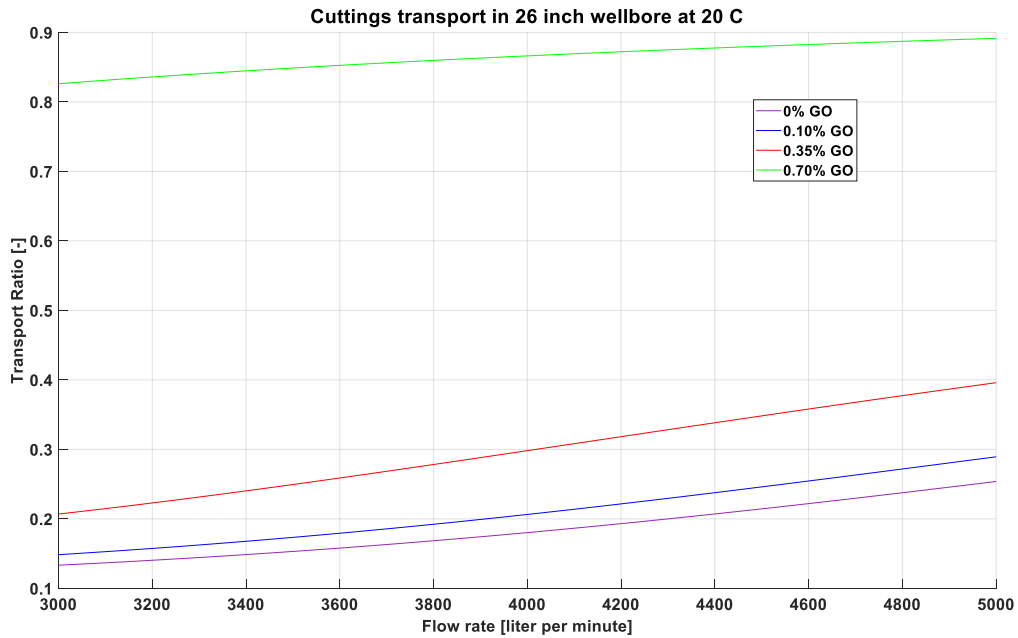


Figure 29. Calculated cuttings transport ratio versus pump rate in 26" casing section for drilling fluids with different concentrations of GO at 20 C.

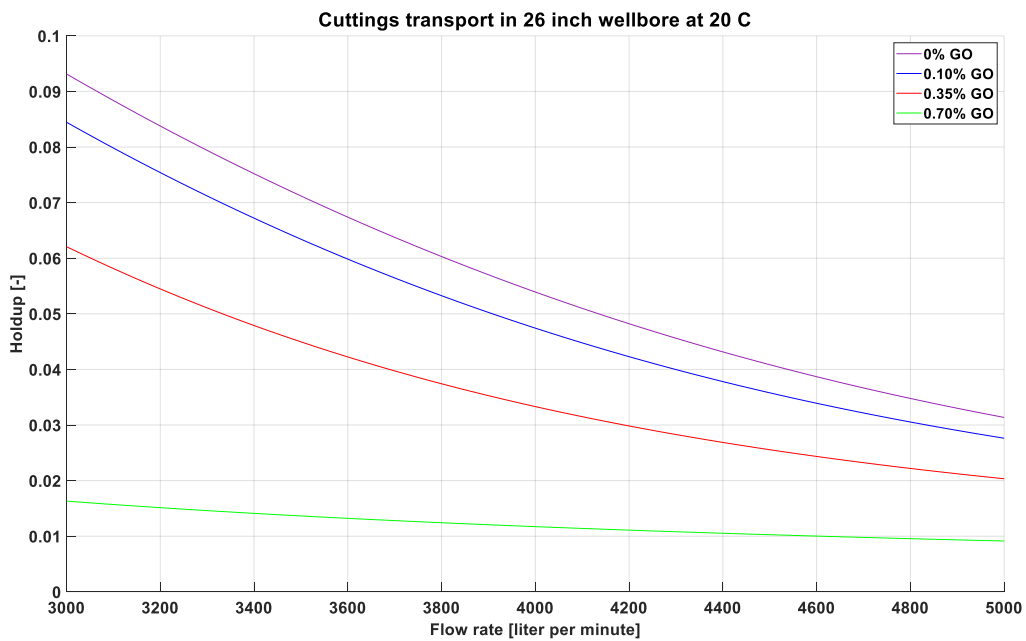


Figure 30. Calculated cuttings holdup versus pump rate in 26" casing section for drilling fluids with different concentrations of GO at 20 C.

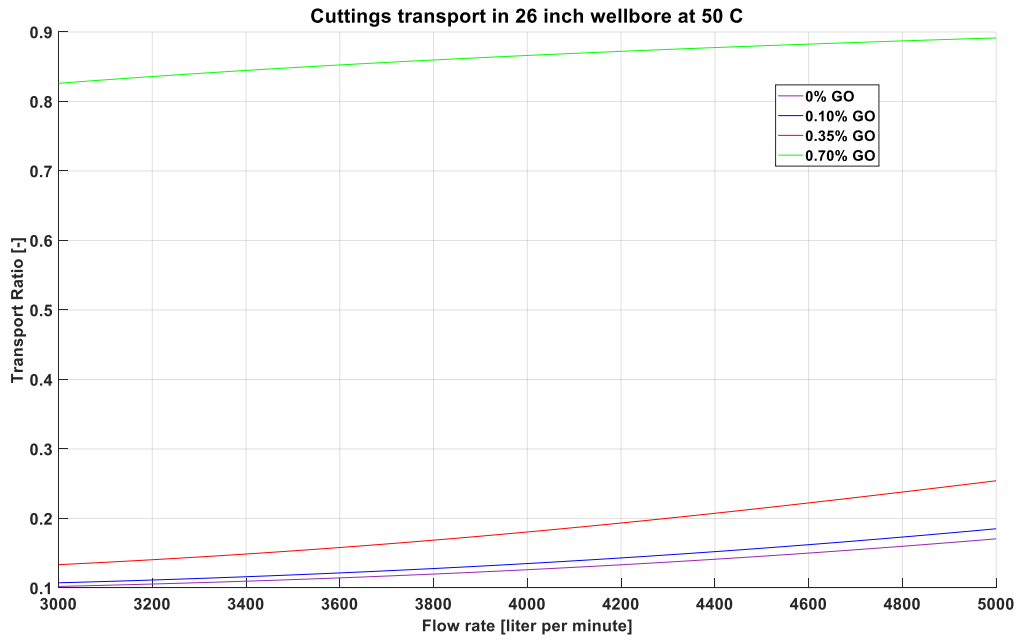


Figure 31. Calculated cuttings transport ratio versus pump rate in 26" casing section for drilling fluids with different concentrations of GO at 50 C.

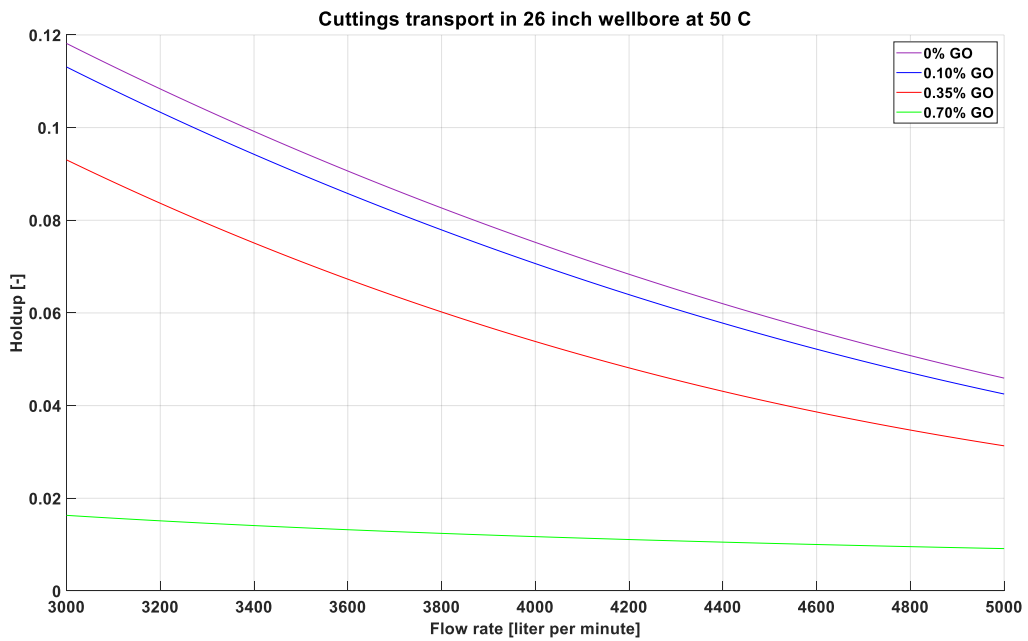


Figure 32. Calculated cuttings holdup versus pump rate in 26" casing section for drilling fluids with different concentrations of GO at 50 C.

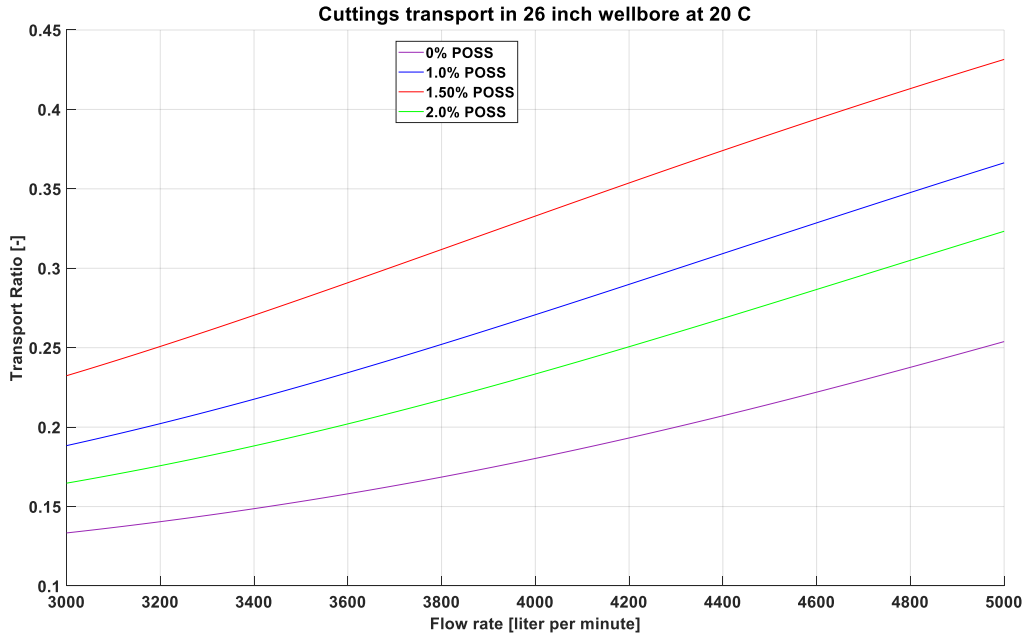


Figure 33. Calculated cuttings transport ratio versus pump rate in 26" casing section for drilling fluids with different concentrations of POSS at 20 C.

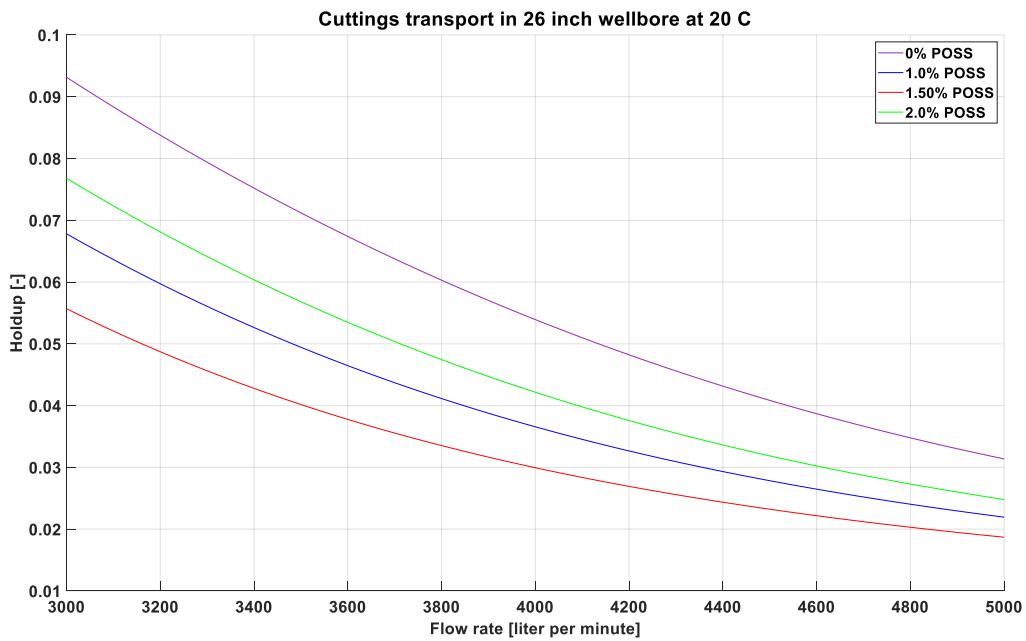


Figure 34. Calculated cuttings holdup versus pump rate in 26" casing section for drilling fluids with different concentrations of POSS at 20 C.

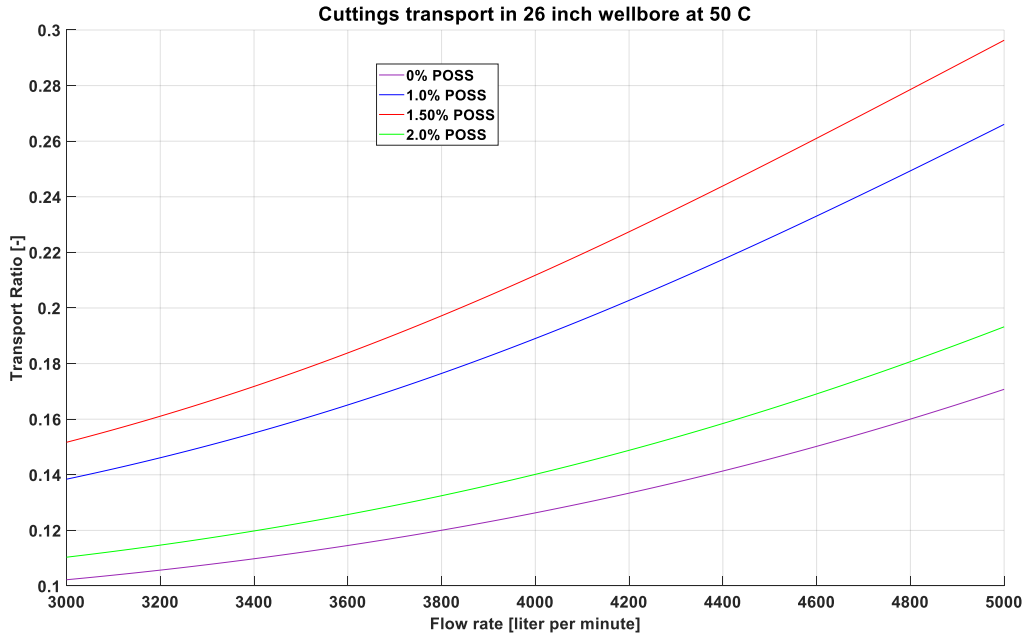


Figure 35. Calculated cuttings transport ratio versus pump rate in 26" casing section for drilling fluids with different concentrations of POSS at 50 C.

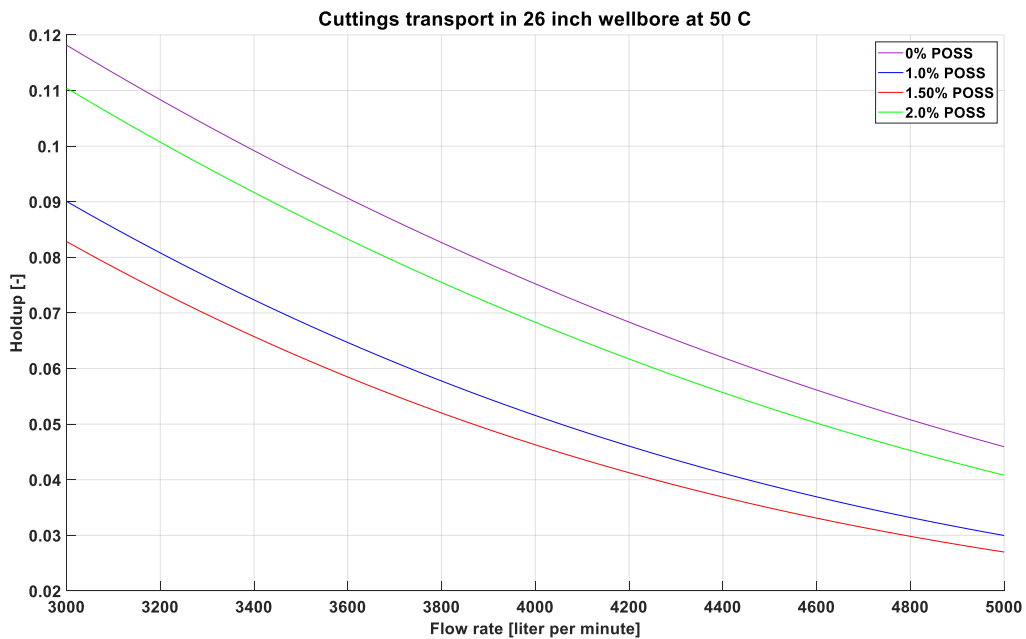


Figure 36. Calculated cuttings holdup versus pump rate in 26" casing section for drilling fluids with different concentrations of POSS at 50 C.

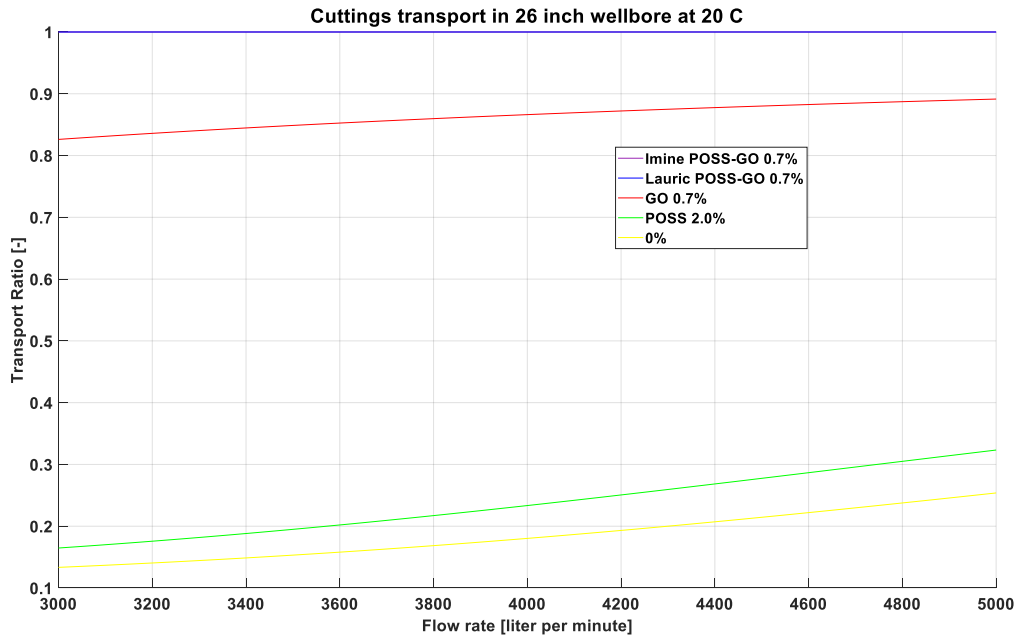


Figure 37. Calculated cuttings transport ratio versus pump rate in 26" casing section for drilling fluids with different concentrations of POSS, GO and POSS-GO at 20 C. Note that the curves for Imine and Lauric POSS-GO are superposed and indistinguishable at unity.

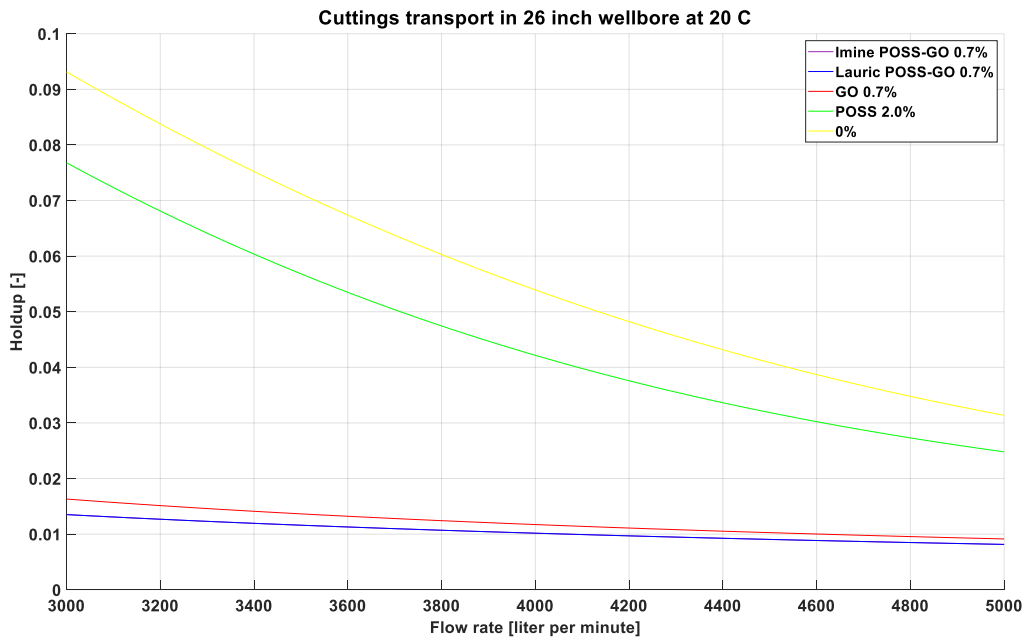


Figure 38. Calculated cuttings holdup versus pump rate in 26" casing section for drilling fluids with different concentrations of POSS, GO and POSS-GO at 20 C. The curves for Imine and Lauric POSS-GO are superposed and indistinguishable due to the transport ratio being unity for these fluids.

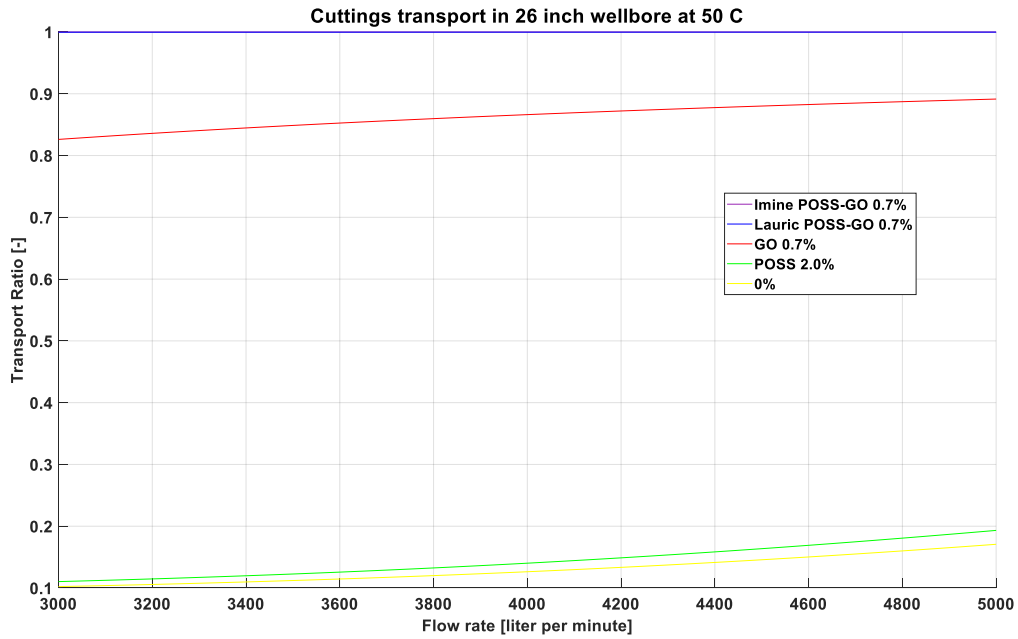


Figure 39. Calculated cuttings transport ratio versus pump rate in 26" casing section for drilling fluids with different concentrations of POSS, GO and POSS-GO at 50 C. Note that the curves for Imine and Lauric POSS-GO are superposed and indistinguishable at unity.

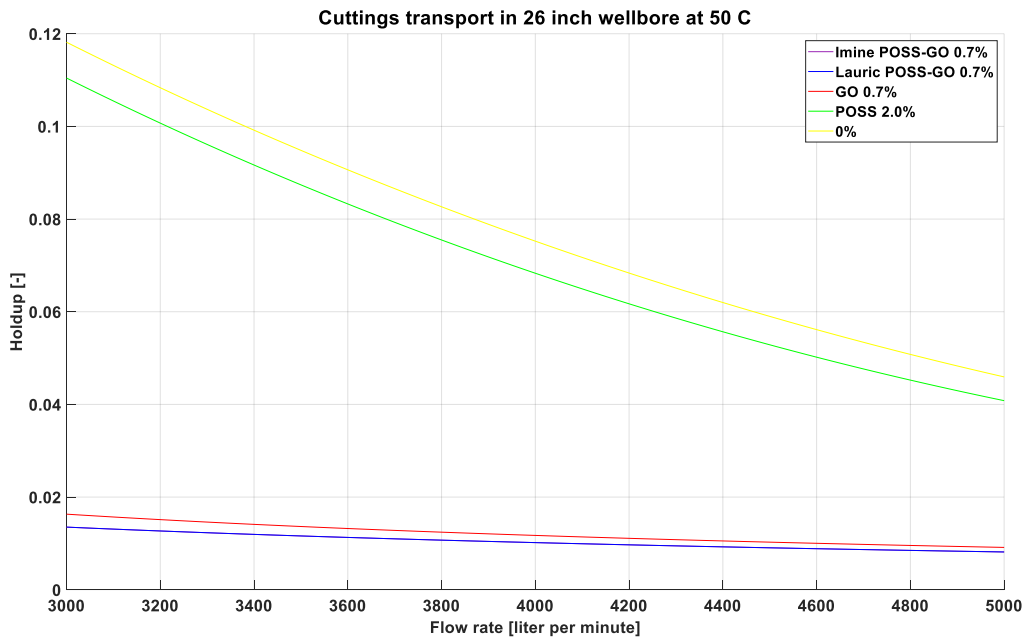


Figure 40. Calculated cuttings holdup versus pump rate in 26" casing section for drilling fluids with different concentrations of POSS, GO and POSS-GO at 50 C. The curves for Imine and Lauric POSS-GO are superposed and indistinguishable due to the transport ratio being unity for these fluids.

6.5 Discussion

From the figures in the previous section, we notice that there is a large difference between the fluids in terms of cuttings transport efficiency, although hole cleaning problems during circulation are not expected in this section for any of the fluids. However, it is important to be aware of the impact of fluid yield stress, which ensures that small particles are kept in suspension also during non-circulation periods. The modified POSS fluids Imine POSS-GO and Lauric POSS-GO have a substantial yield stress, even at 50 C, while the other fluids have negligible yield stress. As a result, these two fluids have a much better particle carrying capacity than the other fluids. In fact, for the assumed particle diameter of 2.7 mm, the settling velocity is virtually zero in these fluids, and the transport ratio is consequently unity with the assumptions made here. However, we notice also that these fluids have a much larger shear stress at large shear rates. Thus, they will also create larger pressure losses compared to the other fluids.

The viscosity and cuttings transport efficiency also appear to increase monotonously with GO concentration, and with a dramatic improvement from 0.35% to 0.7% concentration. In contrast, the POSS additive gives little improvement to viscosity and thus to cuttings transport efficiency. Moreover, the dependency is not monotonous.

Although the particle settling velocity is a good indicator for the velocity required to ensure sufficient cuttings transport. However, Sifferman et al. [7] found that observed transport was 75 to 90% of the theoretical values. Thus, actual transport efficiency for the cases considered could be lower than reported here.

7 Conclusion

Hybrid Nanosilica nanoparticles have been used to functionalize Graphene Oxide. The chemical functionalization on GO (also confirmed by TEM/EDS analysis), is expected to improve the adhesion of the POSS-GO on the surface and to form a protection layer against further wear. The highest reduction in the coefficient of friction was measured with the use of POSS-GO nanoparticles and was correlated with reduction in the wear track examined (3D analyses) after Pin on Plate tests.

An increase in viscosity was also observed with the functionalized additives (POSS-GO) compared to reference drilling fluid, the one with GO and the one with POSS alone. Though functionalized POSS modified GO increased the viscosity of the drilling fluid and the biggest reduction in friction. However, the synthesis process shall be further investigated in order to improve the scalability and reduce the production cost.

Therefore, we have selected lactamide, POSS which also reduce the friction significantly, for scaling up for use in BRI pilot tests that will be performed at Amines laboratory. Nearly 2.2 Kgs Lactamide POSS were produced and sent to Amines test site in Pau, France.

The potential for increased drilling tools life and an efficient jetting has thus been prioritized in the selection of a POSS-based drilling fluid for further BRI pilot tests and to improve the overall drilling performance.

However, in the context of deep geothermal HPWJ and percussive drilling applications, it was pointed out that the potential of these nanoparticles-based drilling fluids should be further assessed (with the "model drilling fluids" used) to address its influence on the cutting transport and the stability of fluids under HPHT.

References

1. Boyou NV., Ismail, I., Sulaiman, W., Haddad, A., Husein, N., Hui, HT. and Nadaraja, K., (2019) Experimental investigation of hole cleaning in directional drilling by using nano-enhanced water-based drilling fluids. *J Petrol. Sci and Eng.* 176, 220-331.
2. Liu F., Jiang GCh, Peng ShP., He YB and Wang JX, (2016) Amphoteric Polymer as an Anti-calcium Contamination Fluid-Loss Additive in Water-Based Drilling Fluids, *Energy Fuels*, 30, 7221-7228.
3. Vryzas, Z. and Kelessidis, V. (2017) Nano-Based Drilling Fluids: A Review. *Energies*, 10, 540.
4. Ma, JY., Pang, SC., Zhang, ZN., Xia, BR., and An, YX (2021). Experimental Study on the Polymer/Graphene Oxide composite as a Fluid Loss Agent for Water-Based Drilling Fluids, *ACS, OMEGA*, 6, 9750-9763.
5. Neubergera, N., Adidharmaa, H., Fan, M. (2018). Graphene: A review of applications in the petroleum industry. *J Petro. Sci. Eng.* 167, 152–159.
6. Rafueefar, A., Sharif, F., Hashemi, A. and Bazargan, A.M., (2021). Rheological Behavior and Filtration of Water-Based Drilling Fluids Containing Graphene Oxide: Experimental Measurement, Mechanistic Understanding, and Modeling, *ACS Omega* 2021, 6, 29905–29920.
7. Sifferman, T. R., Myers, G. M., Haden, E. L., and Wahl, H. A., 1974, "Drill Cutting Transport in Full Scale Vertical Annuli," *Journal of Petroleum Technology*, 26(11), pp. 1295–1302.
8. R. Byron Bird, Warren E. Stewart, and Edwin N. Lightfoot, 2002, *Transport Phenomena*, Wiley International.
9. Brzinski, T. A., and Durian, D. J., 2018, "Observation of Two Branches in the Hindered Settling Function at Low Reynolds Number," *Physical Review Fluids*, 3(12), p. 124303.
10. Saasen, A., and Ytrehus, J. D., 2020, "Viscosity Models for Drilling Fluids—Herschel-Bulkley Parameters and Their Use," *Energies*, 13(20).